# LOCALIZATION OF PACLITAXEL

A Major Qualifying Project

Submitted to the Faculty of Worcester Polytechnic Institute
in partial fulfillment of the requirements for the Degree in Bachelor of Science
in
Chemical Engineering
By


_____

Lexi Crowell

_____

Margaret LaRoche


Date: 22 March 2018

Project Advisor:

_____

Professor Susan Roberts, Advisor

# TABLE OF CONTENTS

# 1. BACKGROUND

## *1.1 The Plant Cell*

Comprised of several different organelles and bound by a complex and penetrable wall, the plant cell is a unique eukaryote that comes in various forms and sizes. The cell wall itself is composed of cellulose, a 14-carbon compound that is difficult to break down mechanically and chemically. Each compartment of the plant cell has a specific and specialized purpose, and while each compartment is fascinating to research, there are two main organelles that are of interest for this research: the plastid and the vacuole (1). The plastid is a double membrane bound organelle that has various subclasses with different functionalities including the chloroplast that supports photosynthesis. The vacuole is also a double membrane bound organelle that primarily consists of water containing inorganic and organic molecules that are hydrophilic. The vacuole usually functions as a vessel that contains waste, water, and harmful materials that may threaten the cell, and is used to maintain turgor pressure in the cell. *Figure 1* depicts the plant cell with its labeled organelles (1).

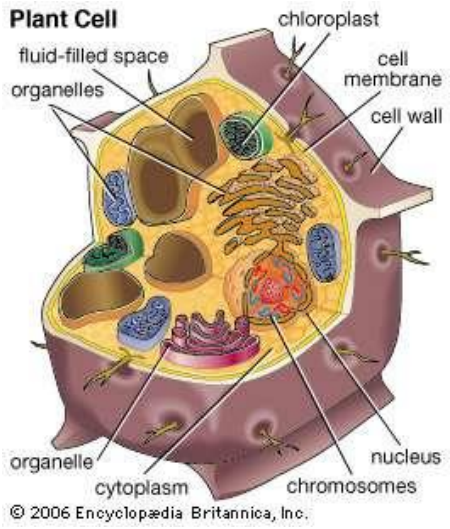


*Figure 1. The plant cell highlighting each organelle (1)*

Most plant cells have similar morphology and their essential biosynthetic pathways are understood; however, in the *Taxus* plant system under study in our laboratory, relatively little is known about cellular metabolism and its compartmentalization. Unlike a traditional plant cell, *Taxus* cells were found to have a variety of plastids including proplastids, leucoplasts, and amyloplasts, each of them derived from one another (2). Using transmission electron microscopy, it was discovered that that proplastids and leucoplasts were formed around the nucleus, and once the cells were mature, the leucoplasts exit the nucleus to the vacuole as shown in *Figure 2.* Since amyloplasts contain starch and leucoplasts contain oil, both hydrophobic compounds, paclitaxel is more likely to be contained in these types of plastids due to its hydrophobicity (2).

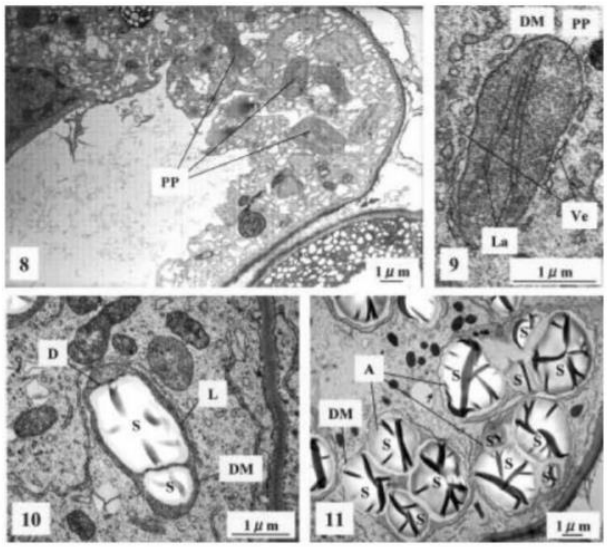


Fig. 8-11: Proplastids (PP), leucoplasts (L) and amyloplasts (A) in callus cells of *Taxus cuspidata* var. nana.
8: The proplastids (PP) before storing the starch grain was observed in young callus cells.
9: These proplastids (PP) were surrounded by a double membrane (DM) and two lamellas (La) were observed clearly and a large number of Vesicles (Ve) stood a line was surrownded by near the exporium of proplastid.
10: The Leucoplasts (L) stored several starch grains (S) wrapped with Double memblane (D) and Leucoplast (L) also wrapped with a double memblane (DM).
11: The amyloplasts (A) stored large number o starch grains (S). These grains did not wrapped with a memblane. However, Amyloplasts (A) were wrapped with a double memblane (DM)

*Figure 2. Transmission Electron Microscopic view of proplastids, leucoplasts, and amyloplasts in callus cells of* Taxus cuspidata *(2)*

## *1.2 Specialized Metabolism in Plants*

While conserved metabolites are essential for plant cellular growth and development and maintenance, specialized metabolites (formerly secondary metabolites) are formed through a separate set of metabolic pathways and are synthesized for various reasons, many associated with induction of a stress response (2). Specialized metabolites aid plants in important functions such as competition, inter and intra species interactions, and UV protection. Specialized metabolites in plants are largely specific to each species, although general classes of specialized metabolites have been classified. Specialized metabolites can be broadly divided into three subgroups: flavonoids, phenolics, and alkaloids (3). Flavonoids, a subsection of phenolics known as bioflavonoids, are comprised of over 5,000 hydroxylated polyphenolic compounds that aid plants with combating environmental stresses such as attracting insects to pollen and regulating cell growth. Their physicochemical properties are crucial to human nutrition because of their metabolic predictability in digestion, absorption, and biotransformation. They exhibit antithrombogenic, anticancer, and neuroprotective activities throughout different *in vitro* and animal models (3). These molecules are commonly found in a variety of fruits and vegetables. Phenolic compounds participate in morphological development and physiological processes. Also known as polyphenols, 8,000 known structures of plant phenolics have been discovered; many are useful in minimizing skin aging, disease, and damage (4). Alkaloids are cyclic organic nitrogen containing compounds that occur in 15% of all land plants. In plants, these compounds typically exist as salts of organic acids and sugars. The nitrogenous element of alkaloids helps protect plants from insects and animals (5).

## *1.3 Introduction to Paclitaxel*

Paclitaxel (Taxol™) is a diterpenoid plant metabolite found originally in the Pacific Yew tree, or *Taxus brevifolia.* The extracts from the bark of the tree demonstrated unique, antitumor behavior

with the potential to treat various types of cancer. In current practices the anticancer compound, paclitaxel, is supplied commercially through plant cell culture technology (6). Paclitaxel is an FDA approved drug for the treatment of numerous cancers, specifically breast, lung, and ovarian cancer.

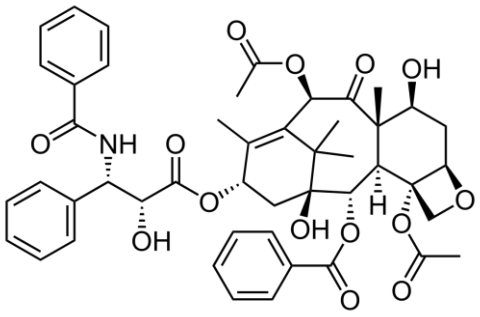


*Figure 3. Chemical structure of paclitaxel (7)*

The chemical name of paclitaxel is 5β, 20-epoxy-1,2α,4, 7β,10β,13α-hexahydroxytax-11- en-9-one4, 10-diacetate 2-benzoate 13-ester with (2R,3S)-N-benzoyl-3-phenylisoserine. The chemical formula is $C_{47}H_{51}O_{14}$ resulting in a molecular weight of 853.918 g/mol. Paclitaxel has a melting point range of 215-217°C (7). The complex structure of the compound makes it difficult to synthesize at scale using traditional organic chemistry methods. Paclitaxel has a cyclodecane structure that is composed of a diterpene, a taxane ring system, an ester side chain, and a four-membered oxetane ring at the C4 and C5 positions as shown in *Figure 3.* The hydrocarbon rings throughout the chemical structure make the molecule hydrophobic, or insoluble in water.

## *1.4 History of Paclitaxel*

Paclitaxel was discovered in 1962 by researchers from the U.S. Department of Agriculture and the National Cancer Institute (NCI). Testing bark extract revealed that the compound had the potential to cure cancer. In 1964, scientists at the Research Triangle Institute's Natural Product Laboratory confirmed that the bark extract exhibits cytotoxic activity. Years later, researchers were finally able to prove antitumor activity in a mouse model, and Dr. Susan Horwitz of the Albert Einstein

College of Medicine discovered that paclitaxel inhibits cell division by stabilizing microtubules and preventing growth (8). Paclitaxel binds to the cell's microtubule assembly and blocks the segregation of chromosomes (9). At the time, this discovery was revolutionary in the field of anti-cancer drugs because the mechanism paclitaxel uses to prevent cell division is extraordinarily different and complex compared to the other antimitotic drugs (10). In 1992, paclitaxel was FDA approved to treat ovarian cancer and approved to treat breast cancer in 1994. While the drug provided great success in cancer treatments, the production of the compound was challenging due to the low yields of inefficient production methods (11). After years of research, plant cell culture emerged as the most efficient commercial production method, beating out chemical synthesis, semi-synthesis from precursors extracted from yew needles, heterologous expression of pathway genes in microbial systems and extraction from natural sources.

## *1.5 Biosynthesis of Paclitaxel*

### 1.5.1 MEP and MVA Pathway

As mentioned previously, paclitaxel is a terpenoid, which is a diverse class of natural compounds that has many functions in human health and nutrition. There are over 40,000 terpenoid structures that have been discovered, with paclitaxel being one of most studied terpenoids (12). Isopentyl diphosphate (IPP) and dimethyl diphosphate (DMAPP) are of significant interest in the formation of the diterpene. As shown in *Figure 4A*, the two precursors form other complex compounds such as the diterpenoid geranylgeranyl pyrophosphate that serve as the starting point for terpenoid synthesis. *Figure 4B* demonstrates the compartmentalization of terpenoid synthesis and highlights the redundancies of pathways that are often observed in plant systems. As research in specialized metabolism increased, scientists began to focus heavily on IPP and DMAPP synthesis and conversion and found that they were part of two distinct metabolic pathways within two distinct compartments of the cell: the mevalonate (MVA) pathway and 2-C-methyl-D-erythritol-4-

phosphate (MEP) pathway. The two pathways are still not well defined; however, evidence has revealed that the two precursors IPP and DMAPP, flux in and out of different compartments of the cell. The two precursors in each pathway have mostly been shown to appear in the cytosol and plastid compartments of a plant cell. The MVA pathway has been of significant interest because IPP can control plastidic terpenoid synthesis. The enzymes in the MEP pathway have been found to influence the rate at which terpenes are formed (12).

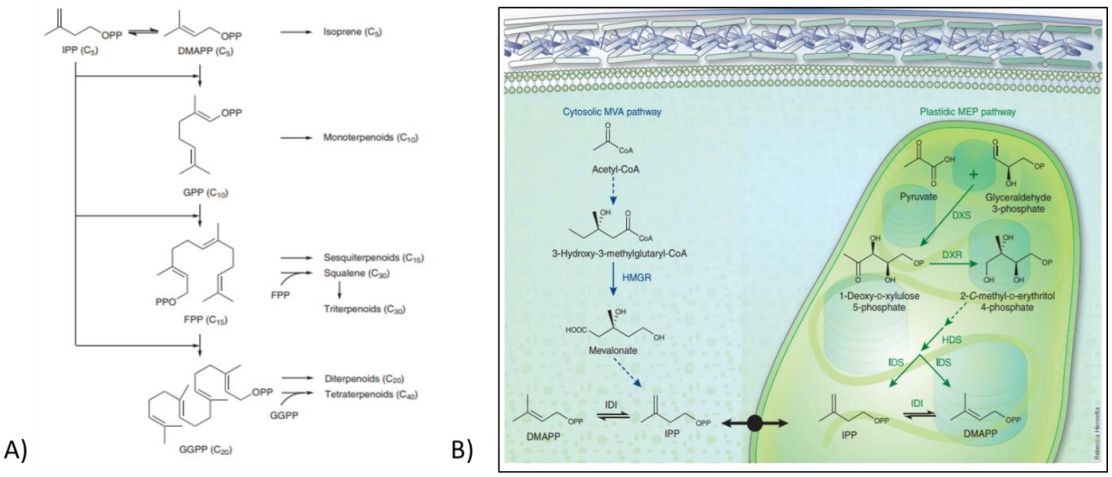


*Figure 4. A) Schematic of the two main precursors in the MEP and MVA pathways B) Depiction of the MEP and MVA pathways within different compartments of the cell (2)*

These two pathways and precursors are of significant interest to scientists and metabolic engineers since the biosynthetic pathway to paclitaxel is still not fully understood. Our project has been designed to better understand the distribution of paclitaxel in these two important compartments. Information on the localization of paclitaxel in the cell will allow researchers to better understand the pathway and design engineering strategies to both increase yield and transport of paclitaxel out of the cell to simplify product purification.

### 1.5.2 Important Taxane Precursors

Paclitaxel is one of a class of molecules called taxanes, all with similar core structures. In the biosynthetic pathway of paclitaxel, there are two precursors that accumulate in the needles of the yew tree as well as in cell culture: baccatin III and 10-deaceytlbaccatin III. Due to their increased accessibility, the two precursors have been heavily studied and efforts have been made to synthesize paclitaxel from these precursors (13). Although the biosynthetic pathway is not fully known, the acetylation of 10-deactyelbaccatin to baccatin III has been studied. The reaction and conversion is highly dependent on the addition of 10-deacetylbaccatin III as is important to the 10-hydroxyl group for the formation of the taxane ring as a product of paclitaxel (13). These two related taxanes are depicted in *Figure 5*. Because of their high industrial importance, these two precursor compounds, along with paclitaxel, are commercially available for purchase, facilitating future studies of precursor location in the cell.

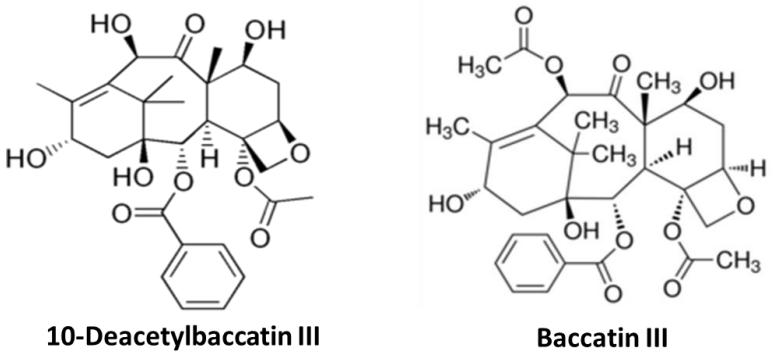


*Figure 5. Chemical structures of 10-deacetylbaccatin III and baccatin III (13)*

### 1.5.3 Paclitaxel Biosynthetic Pathway Enzymes

The biosynthesis of paclitaxel is estimated to be a 19-step process. While not all steps are known, there are 9 main steps that have been identified. From the MVA or MEP pathway, the next step is production of geranylgeranyl diphosphate, which is then cyclized to form taxadiene. This step

establishes the taxane skeleton followed by oxidation shown in *Figure 6*. The C9 in the intermediate step is oxidized, forming baccatin III, which is hydroxylated and benzoylated to yield the final product of paclitaxel (14)

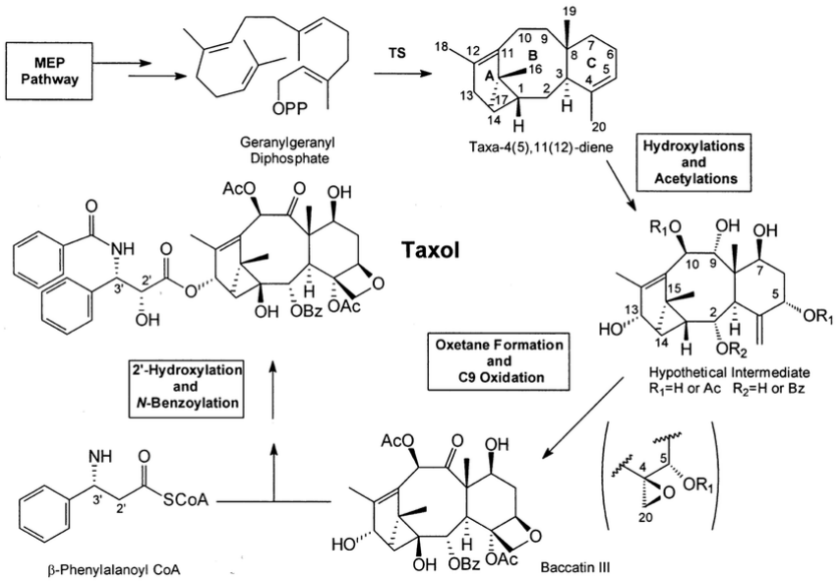


*Figure 6. The known steps in the paclitaxel biosynthetic pathway (13)*

## *1.6 Paclitaxel Production Methods*

### 1.6.1 Harvest and Bark Extraction

The first method to obtain paclitaxel was by crude extraction from the bark of the Pacific Yew tree. To obtain the extract from the bark, researchers used solvent extraction and combined bark stripped from the *Taxus* tree in solution with methanol (7)**.** Because *Taxus* grows at a slow rate, a tree must be at least 80 years old to provide enough bark and paclitaxel to undergo bark extraction for crude product (15). *Figure 7* depicts a picture of the Pacific Yew tree and associated needles. The slow growth rate coupled with the low yield of paclitaxel makes bark extraction an unsustainable method for paclitaxel production. The low yield from the bark is best illustrated in the preparation for the first clinical trial at the National Cancer Institute (9). Researchers and clinicians were able to acquire approximately 60,000 lbs of bark from the Pacific Yew tree but

were only able to extract 9 lbs of paclitaxel in the crystalline form (15). The low yield disappointed researchers, as it was not enough to conduct even the first phase of the clinical trials. Continuation of such research drew negative attention from environmentalists as the tree neared endangerment as a species, forcing the NCI to acknowledge that crude extraction was not a feasible method. Due the many challenges of low yields, the negative environmental impact, and the large amount of space needed to grow the necessary number of trees, researchers continued to investigate other methods for paclitaxel production that would allow them to conduct clinical trials.


*Figure 7. A) Largest pacific yew found in Seattle, WA B) Needle of* Taxus brevifolia *tree where 10-deacetylbaccatin III and baccatin III accumulate*

### 1.6.2 Total Organic Synthesis

While paclitaxel can be extracted and produced from bark extract, in its early discovery, researchers searched for other methods of production. In 1994, K.C. Nicolaou and colleagues at the University of California San Diego discovered and published the first method to fully synthesize paclitaxel (16). Despite their success, researchers concluded that the steps to synthesize paclitaxel were far too complex, utilize harsh chemicals, and are too expensive to produce the anticancer drug at scale. *Figure 8* shows the formation of the C-Ring and A-Ring via the Nicolaou synthesis method. The synthesis of the C-ring includes 10 steps to construct the complex C-ring while the A-ring structure includes four steps. The complexity of this synthesis drove researchers

to investigate other ways to synthesize paclitaxel that would be less expensive, faster, and more environmentally sound. Overall, these methods produce lower yields, making it difficult to obtain adequate amounts of paclitaxel for production and supply (6).

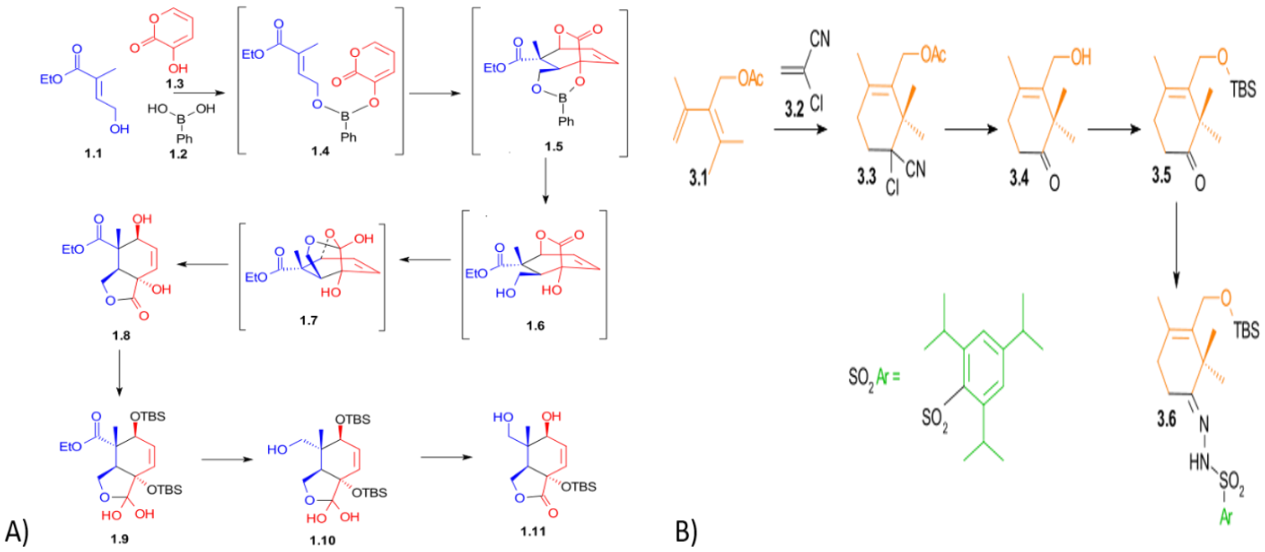


*Figure 8.* A) *C-ring semi-synthesis via Nicolaou synthesis,* B) *A-ring synthesis via Nicolaou synthesis (16)*

### 1.6.3 Semi-Synthesis

Another approach to synthesize paclitaxel is through semi-synthesis. This process was first used after it was discovered that two precursors of paclitaxel, baccatin III and 10-deacetylbaccatin III could be found in large amounts in the needles of the tree, a fast growing and renewable part of the plants. These diterpenoid taxanes have a similar structure to paclitaxel (9) and can be converted to paclitaxel in the laboratory. Because extraction from needles eliminates the step of sacrificing an entire tree, the semi synthesis process has been used to synthesize paclitaxel as well as related taxanes, shown in *Figure 9* (10). However, because the semi-synthesis method used several harsh solvents, it was eventually deemed too environmentally toxic for continued supply of paclitaxel.

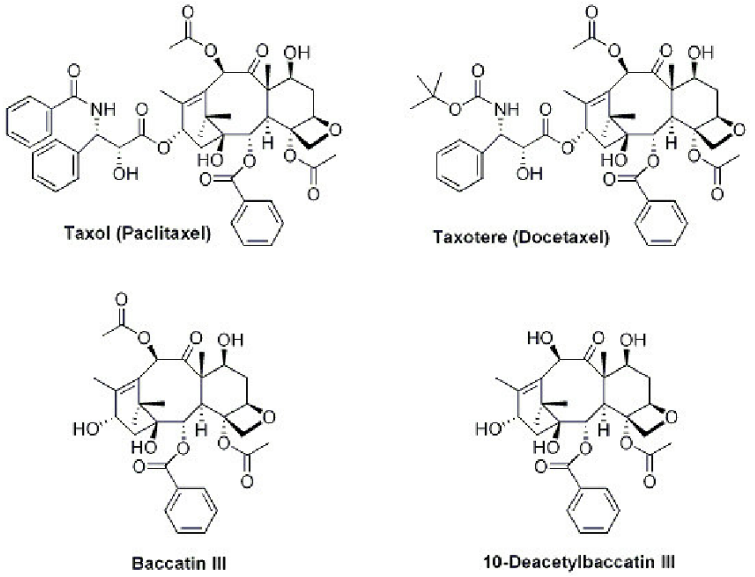


*Figure 9. The chemical structures of different taxanes (17)*

### 1.6.4 Heterologous Expression

Researchers have discovered a large part of the paclitaxel biosynthetic pathway and have investigated heterologous expression of the pathway in bacteria and yeast. Scientists began with expressing taxadiene synthase (the first committed step in the paclitaxel pathway) in alternate systems. For example, a functional taxadiene synthase from *T. chinensis* was successfully expressed in *S. cerevisiae*; however, an insufficient amount of GGPP was available to support synthesis (18). Although the entire biosynthetic pathway has yet to be identified, individual enzymes in the pathway have also been expressed in microbes (19).

### 1.6.5 Plant Cell Culture

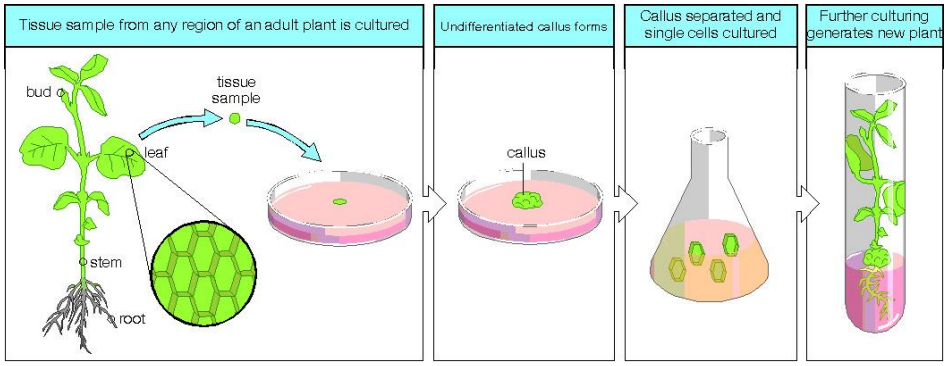


*Figure 10. Process of how plant cell culture is initiated in three steps: tissue extraction, callus culture, and lastly cell suspension (20)*

It has been determined that the most cost-productive and time efficient way to produce paclitaxel is through plant cell culture. The process, unlike the other production methods, is sustainable and provides the opportunity to increase yields through strategic manipulation. *Taxus* plant cell culture utilizes less environmentally toxic compounds and reduces byproducts that could potentially harm the environment (15). Cells are suspended in a liquid media (i.e., suspension culture) and can produce paclitaxel as well as other compounds that the plant may not synthesize in nature, shown in *Figure 10*. Plant cell culture has many advantages, including the ability to manipulate any physio-chemical and physiological environmental parameters as well as the ability to monitor and study the production of specialized metabolites. Plant cell culture has been used since the 1950s, and its use has continually increased, especially with the development of advanced bioreactors (16). Although plant cell culture is the best current option for paclitaxel production, the process is still lacking optimization. For example, certain cell lines can have as little as a 7-10% of the total paclitaxel released into the cell media (17). To increase the yield of paclitaxel in our system, an "elicitor" is added to the culture medium. Elicitors are compounds that can activate specialized metabolism through inducing a stress response resulting in increased expression of genes involved.

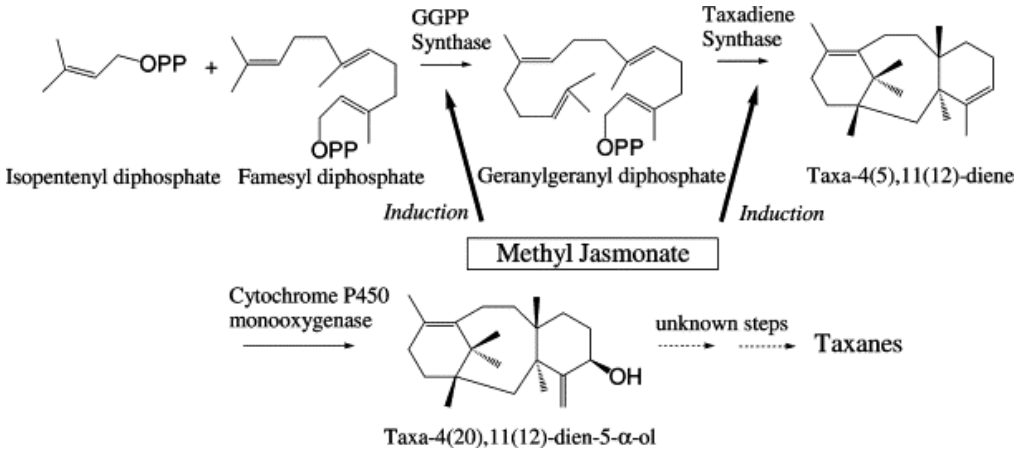


*Figure 11. The biosynthetic pathway of paclitaxel with the addition of the elicitor methyl jasmonate, which induces regulation of GGPP synthase and taxadiene synthase (21)*

In *Taxus* cell suspension, methyl jasmonate, a plant hormone, can induce specialized metabolism, including increasing yields of 10-deacetylbaccatin III, baccatin III and other taxanes such as paclitaxel (18) (*Figure 11*). While elicitation increases the production of specialized metabolites through upregulation of the relevant biosynthetic pathways, product yields can still be improved (21). To gain a better understanding of why secretion of paclitaxel into the extracellular medium is low, the transport of paclitaxel both within and outside of the cell should be investigated. Localization of paclitaxel within the plant cell will allow for optimization of secretion to increase transport to the extracellular media and later improve downstream processing.

## *1.7 Paclitaxel Transport in Cell Culture*

Several studies were conducted to determine how paclitaxel is transported in the cell and out of the cell to either the cell wall or medium compartments. Studies with competitive inhibition suggested that only paclitaxel could inhibit the cellular uptake of itself, indicating that the transport mechanism for paclitaxel likely discriminates between paclitaxel and related taxanes with similar structures (17). This specificity suggests that there is a specific transport protein allowing the movement of the hydrophobic compound across the cell membrane. Identification of this protein is critical to future engineering research of paclitaxel transport. Reports have shown that

extracellular secretion of paclitaxel can range from 10% in *T. x media* suspension cultures to nearly 90% in *T. baccata* suspension cultures (22). Researchers have been working to develop more specific strategies to increase secretion of paclitaxel to the cell media. To complete this goal, we must understand not only the paclitaxel transport mechanism, but also determine where paclitaxel is located in the cell (23).

## *1.8 Method Development: Summary of the Different Approaches Employed in this MQP*

### 1.8.1 Approach I: Localization using Digestion Enzymes & Fractionation

Multiple studies have attempted to determine the intracellular location of paclitaxel. One study used cell wall digesting enzymes to determine the content of paclitaxel and found that most of the cell-associated (i.e., either intracellular or localized to the cell wall) paclitaxel was located in the cell wall matrix or within the space between the cell wall and plasma membrane (24). In *T. chinensis* culture, about 50% of the paclitaxel was localized to the cell-associated fraction. Studies using *T. cuspidata* suspension cells in both growth and stationary phases showed that 30-35% of the paclitaxel was cell-associated. For cells grown in solid culture (i.e., callus), 30% of paclitaxel was cell-associated in exponential growth phase cells as opposed to 43% in stationary phase cells (25).

Studies were conducted on *T. chinensis* suspension cultures to further resolve the cell-associated fraction of paclitaxel. Results showed that 54.8% of paclitaxel was in the cell wall, 25.3% was inside the plastids or nuclei, 4.8% inside starch grains, 3.2% in ER and microsome, and 11.9% inside smaller particles (26). Cell cultures were homogenized and sampled using HPLC to quantify the amount of paclitaxel in each fraction. Dry cells were homogenized with a mortar and pestle in chilled Tris-HCl buffer. The homogenate was then filtered through a 40μm mesh and washed with Tris-HCl buffer and water to separate the cell wall fraction from the intracellular components. The

intracellular components were immersed in the same buffer and separated based on differential centrifugation. This cell homogenization technique was adapted and used in this MQP to further explore intracellular paclitaxel localization.

### 1.8.2 Approach II: Localization using Histology

In the 1995 study that used immunocytochemical methods to localize paclitaxel in *Taxus cuspidata* (26), researchers found that many of the methods they tried failed due to difficulties with traditional histological techniques. For example, when trying to use antibodies that would bind to paclitaxel, they found that the available antibodies did not have the ability to differentiate between the different taxanes (e.g., paclitaxel and baccatin III), hence complicating localization studies. In addition, they found that paclitaxel was soluble in most solvents that are used to fix and dehydrate microscopy samples (25). Hence, histological studies need to be carefully designed and results verified to ensure that paclitaxel is not mobile during sample preparation.

### 1.8.3 Approach III: Localization using Subcellular Fractionation

To determine the distribution of subcellular metabolites in *Arabidopsis thaliana* leaf tissue, researchers utilized a procedure that we adapted here for paclitaxel localization. The methods from the *A. thaliana* leaf tissue are applicable here because of the focus on quantification of enzymes in the plastids, vacuole, and cytosol (27), to ensure sufficient compartment separation. Cell lyophilization and homogenization were used prior to fractionation. The lyophilization process freeze dries the cells and allows them to be homogenized and stored for subsequent experiments. Because paclitaxel synthesis is known to occur in both the cytosolic and plastidic compartments, the quantification of paclitaxel in these cell organelles is important to understand cell localization.

### 1.8.4 Approach IV: Localization by Subcellular Fractionation and Ultracentrifugation

A procedure for ultracentrifugation followed by a sucrose gradient was adapted from a National Institute of Health (NIH) study on mammalian cell fractionation (1). Utilization of a sucrose gradient works best with organelles or particles that differ greatly in size. To gain a better separation, the sucrose is used to create a density gradient that separates components into distinct bands. The sucrose gradient method was adapted and used to separate the intracellular components of *Taxus* cells after they had been lyophilized and homogenized (28).

# 2. INTRODUCTION TO THE MAJOR QUALIFYING PROJECT

The purpose of this MQP is to develop and implement methods to determine where paclitaxel is stored and produced in *Taxus* cells. This research is significant to the broader goal of paclitaxel production optimization in that research will inform engineering strategies to increase secretion to extracellular media. This MQP can be divided into four parts: cellular fractionation, organelle analysis through assay development, quantification of paclitaxel, and finally the combination of the data to determine paclitaxel localization. The first objective was to ensure that the cells are properly cultured, elicited, lyophilized, and lysed to accomplish cellular fractionation. The second objective was to analyze the cell fractions and determine where the two main organelles significant to this research, the plastid and vacuole, are located within the sucrose gradient. Although it is suggested in literature that paclitaxel is not produced or found in the vacuole, it is important to verify there is no paclitaxel located in the vacuole because the vacuole is a typical storage site for specialized metabolites in plant cells. The presence of the two organelles in distinct fractions was determined using different enzyme assays. Because alkaline pyrophosphatase is stored in the plastid, an enzyme assay that tests the abundance of alkaline pyrophosphatase was developed and used to confirm the presence of plastids in the cellular fractions. Acid phosphatase is an enzyme that is found in the vacuole and was used to quantify vacuole activity (28). The third objective was to analyze which fractions contain paclitaxel using ultra-performance liquid chromatography (UPLC). Since plastids store and manufacture metabolites for the cells, we hypothesized that the concentration of paclitaxel in this fraction will be highest. Due to the hydrophobic nature of paclitaxel, we did not expect to see paclitaxel in the vacuole-rich fraction. Because plastids are less dense than vacuoles it was hypothesized that the amount of alkaline pyrophosphatase would be highest in the lower density sucrose fractions. Conversely, the acid phosphatase concentration

was hypothesized to be greatest in the higher density sucrose fractions. *Figure 12* shows the hypothesized distribution of alkaline pyrophosphatase, acid phosphatase, and paclitaxel throughout the sucrose gradient.

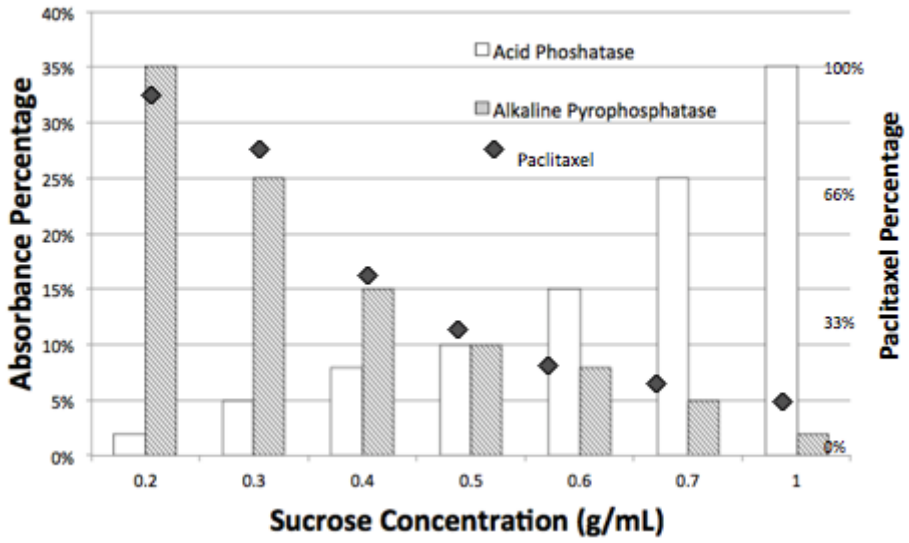


*Figure 12. Hypothetical results expected from both enzyme assays and UPLC analyses*

# 3. METHODOLOGY

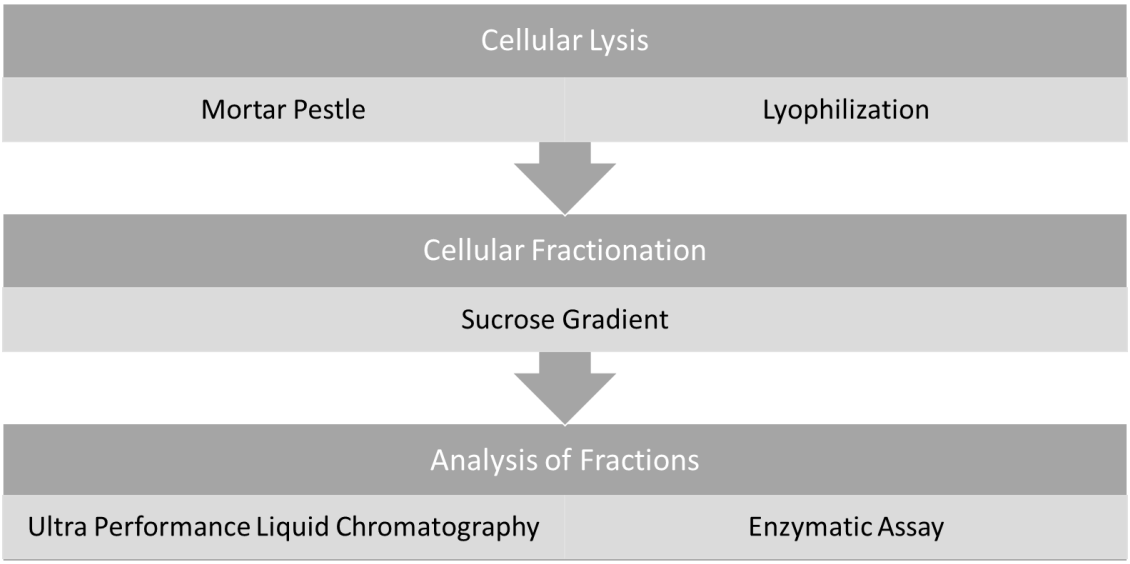


*Figure 13. Schematic of the methodological process for localization of paclitaxel*

## *3.1 Maintaining Plant Cell Culture*

The cell line used in this study was *T. chinensis* line 48-82A-4. Cells were suspended in an aqueous solution containing 20 g/L of sucrose, 3.21 g/L Gamborg's B5, $8.3\times10^{-3}$M BA, and $1.03\times10^{-3}$M NAA. 40 mL of cell media was measured into 125 mL flasks, which were autoclaved at 121ºC for 3 minutes to ensure the sterility of the media and flask. Antioxidants were prepared sterile with $1.42\times10^{-3}$M ascorbic acid, $1.3\times10^{-3}$M citric acid and $9.99\times10^{-3}$M L-glutamine. 2.5 mL of antioxidants and 10 mL of cell suspension (cells plus conditioned media; approximately 10 mL of cells and 40 mL of media) were transferred to each flask, to ensure that the cells remained healthy and viable for experimentation. The flasks containing cells were cultured in the dark at ambient temperature on an orbital shaker at 125 rpm, and subcultured every 14 days to ensure their longevity and viability. For experimentation, cells were elicited on day 7 with 200 µM methyl jasmonate. On day 14 or 21 cultures were tested for paclitaxel using standard UPLC methods in

our laboratory. On day 15 or 22 cells were harvested via vacuum filtration in a Buchner funnel. The cells were put into 15mL Falcon tubes to prepare for subsequent lyophilization.

### *3.2 Lyophilization and Cell Lysis*

*Lyophilization.* A benchtop lyophilizer (Sp Scientific) was used to freeze dry the cells. Before use, the machine was defrosted and brought to operating -30 to -40°C temperature and 100 -200 mTorr pressure. The suspended cells were obtained from the incubator and the media removed via vacuum filtration. Cells were then rinsed with 0.1 M phosphate buffered saline (PBS) three times, utilizing the vacuum filtration to remove excess PBS. 15 mL of dried cells were added to 50 mL polycarbonate Falcon tubes. Before connecting to the lyophilizer, the Falcon tubes were dipped in liquid nitrogen to snap-freeze the cells. The tube was then connected to the lyophilizer and the lyophilizer was run for 8-10 hours. Freeze dried cells were stored at -80ºC until ready for use (27).
*Cell Lysis.* Lyophilized cells (0.1 g) were added to 3 mL of PBS. The mixture was lysed using mortar and pestle for approximately 5 minutes. To ensure that cells were efficiently lysed, homogenized solutions were observed under a light microscope. Once properly lysed, the mixture was added to the sucrose gradient using a 1 mL pipette.

### *3.3 Cellular Fractionation*

To achieve separation of the cellular components, procedures developed and published from the University of California at Davis and the NIH were adapted and combined (28). To determine the concentration of sucrose that would be best for *Taxus* cells used here, different solutions of sucrose concentrations were made. Each sucrose layer was prepared in a 50 mL flask using PBS as the solvent. All sucrose mixtures were heated for 1 minute using a microwave to supersaturate the solutions and dissolve the large amount of sucrose. The ultracentrifuge tubes were stored at 4°C for one hour before combining to create a sucrose gradient. From heaviest on the bottom to lightest

density on top, 1 mL of each layer was pipetted into a 10.3 mL Beckman polycarbonate ultracentrifuge tube. The sucrose gradient was then stored at 4°C for 12-16 hours (28). 1 mL of the processed cells (described above) was added to the top of each ultracentrifuge tube. This was done very carefully to allow the lysed cells to slowly enter the sucrose gradient. Once the cells were layered on top of the sucrose gradient, the sample was centrifuged at 50,000 rpm for 4 hours in the Beckman Coulter ultracentrifuge (1). After ultracentrifugation, the tubes were stored at 4ºC for 2 hours. After the refrigeration period, a pipette was used to separate each 1 mL layer. Each fraction was compiled with the other fractions of the same density from replicate ultracentrifuge tubes to provide a larger volume to work with. Once compiled, the fractions were aliquoted into 1 mL samples to be tested using each assay (see below). The results from these experiments were used to determine which sucrose layer would be best for separating *Taxus* cell components.

### *3.4 Alkaline Pyrophosphatase Enzymatic Assay*

All reagents in this assay were prepared fresh for each use. A stock solution of 40 mM Tris-HCl at pH 8.5 was prepared and brought to the correct pH by adding NaOH. The assay buffer was prepared with 1 mM of $Na_4P_2O_7$, 5 mM $MgCl_2$, 100 mL of Tris-HCl. In a centrifuge tube, 450 µL of buffer solution was added to 50 µL of cell lysis and incubated in a controlled room at 37ºC for 2-4 hours until a color change was observed. 250 µL of ice cold 10% trichloroacetic acid was added to the mixture to stop the reaction. Then 100 µL of the sample was added to a 96-well plate to measure the absorbance between 405-414 nm using Fisher Scientific AccuskanGO microplate reader. This assay was used to quantify the plastid presence in each sucrose layer (29).

### *3.5 Acid Phosphatase Colorimetric Assay*

Acid Phosphatase Colorimetric Assay Kit (Cayman Chemical #10008051) was utilized to quantify the vacuole presence in each sucrose layer. The kit was stored at 4ºC away from any light exposure. The working solution of the assay buffer was prepared with 1.67 mL of acid phosphatase buffer and diluted with 15 mL of nanopure water and stored at room temperature. Acid phosphatase substrate solution was prepared with one tablet of p-nitrophenyl phosphate (*p*NPP) dissolved in 1.5 mL of Assay Buffer and stored on ice. Acid phosphatase stop solution was prepared with 2.0 M NaOH diluted to 15 mL of nanopure water. In a centrifuge tube, 100 µL of buffer solution was added to 50 µL of cell lysis and incubated in a controlled room at 37ºC for 12-15 hours until a color change was observed. After incubation, 100 µL of stop solution was added to the mixture. 100 µL of the sample was added to a 96-well plate to measure the absorbance between 405-414 nm (30) using Fisher Scientific AccuskanGO microplate reader.

### *3.6 Extraction of Paclitaxel*

Before the samples could be analyzed for paclitaxel, a method for extraction of paclitaxel from the sucrose layers needed to be developed. Prior research has shown that the best way to extract paclitaxel is via a methanol rinse. The procedure used was adapted from the Roberts laboratory general procedure for paclitaxel extraction from culture broth using methanol. 1 mL well-mixed samples were placed into a 1.5 mL centrifuge tube and dried in the evaporative centrifuge (Eppendorf Vacufuge Concentrator) for approximately 6 hours. The evaporative centrifuge was set to the V-AQ setting and the condensation trap was placed on ice to accelerate the process. Once the aqueous layer was evaporated, the pellet was resuspended in 1 mL acidified methanol (0.01% acetic acid in MeOH). To effectively mix the methanol with the sample to extract paclitaxel, a combination of mixing techniques was used such as incubation via hot water bath, and sonication via water bath. These mixing techniques were performed between 2-3-minute time intervals and

repeated if mixing did not occur. To ensure that the paclitaxel completely separates from the cell matter, the samples are also manually broken up using a small spatula and then centrifuged for 20 minutes at 15,000 rpm. After centrifugation, 800 µL of supernatant were removed and transferred to a 1.5 mL centrifuge tube. The samples were then placed into the evaporative centrifuge again and dried for approximately one hour. Samples were then resuspended in a mixture of 25 µL methanol, 35 µL acetonitrile, and 40 µL water and sonicated in a water bath for approximately one minute. The samples were then vortexed to assure that each sample was completely dissolved. Once dissolved, each sample was syringe filtered through a 0.22 µM polyvinylidene fluoride (PVDF) filter into a low-volume UPLC vial (Thermo Fisher Scientific 11 mm Clear Glass Crimp Top Vial [Catalog Number C4012-1W]). The samples were then stored at -80℃ until UPLC quantification.

### *3.7 Quantification of Paclitaxel Using UPLC*

UPLC was used to quantify paclitaxel, baccatin III, and 10-deacetylbaccatin III in different cell fractions. Authentic standards were prepared for comparison with retention time and UV spectrum. 1 mg of each authentic compound was measured and placed into a 1.5 mL microcentrifuge tube. 1 mL of methanol was added, and the sample mixed via vortexing to create a 1 mg/mL stock solution. The standard set was created by first diluting with 70:30 water and acetonitrile at a volume of 500 µL in a 1.5 mL centrifuge tube as shown in *Table 1*.

*Table 1. Concentrations of Water and Acetonitrile needed for UPLC Samples*

| Concentration (mg/L) | Stock Solution (µL) | 70:30 water/acetonitrile (µL) |
|---|---|---|
| 0 | 0 | 500 |
| 10 | 5 | 490 |
| 25 | 12.5 | 487.5 |
| 50 | 25 | 575 |
| 75 | 37.5 | 462.5 |
| 100 | 50 | 550 |
| 150 | 75 | 525 |

Each standard was then syringe filtered through a 0.22 µM PVDF filter into a low-volume UPLC vial. The standards were run under the same conditions and at the same time as the experimental samples under the conditions listed in *Table 2*. These standards were used as reference points for the experimental data. All standards and samples were injected into the UPLC at a 10 µL injection volume. The UPLC was set to run with two different solvents – water and acetonitrile.

*Table 2. UPLC parameters for flow rate, time, and solvent composition*

| Time (minutes) | Flow (mL/min) | %Water | %Acetonitrile |
|---|---|---|---|
| Initial | 0.500 | 70% | 30% |
| 0.05 | 0.500 | 70% | 30% |
| 4.50 | 0.500 | 20% | 80% |
| 5.00 | 0.500 | 70% | 30% |
| 6.00 | 0.500 | 70% | 30% |

The pressure limits were set to be 10,000 psi for the high and 0 psi for the low. Once the UPLC run was complete, results were analyzed to determine which fraction yielded the highest concentration of paclitaxel, baccatin III, and 10-deacetylbaccatin III by comparison against the standard curve. An example chromatograph for a standard sample is shown in *Figure 14.* A standard curve is created for each individual compound using the data from the standard run trials. To create the standard curve, a plot is generated with the x-axis representing the concentration of the standard ($\frac{mg}{L}$) and the y-axis representing the area under the peak ($uV \times s$). The line of best fit is determined from the plot ensuring that the y-intercept is set to 0.

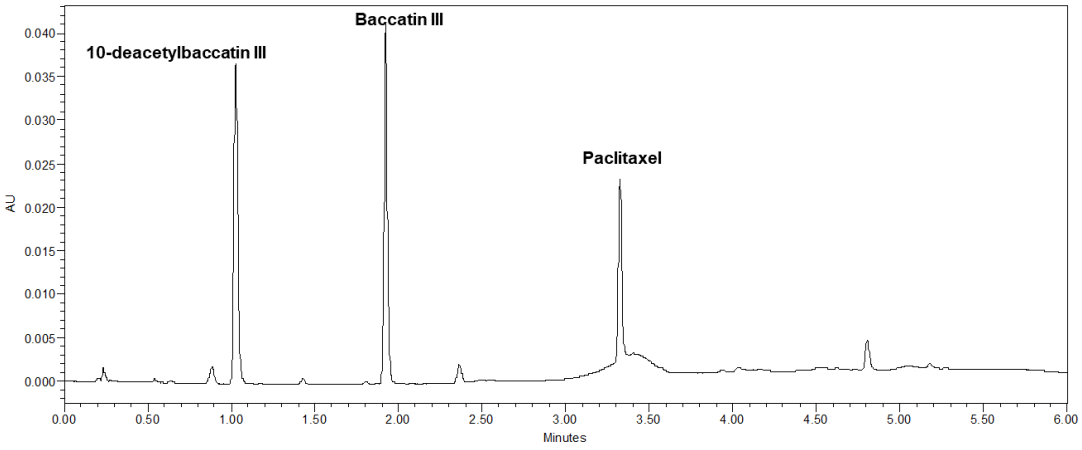


*Figure 14. Chromatogram showing elution times of 10-deacetylbaccatin III, baccatin III, and paclitaxel*

Once the standard curve is created, the concentration of each sample can be calculated using the linear equation of fit. The final concentrations of the samples are determined by dividing the calculated concentration by eight because the samples were concentrated eight times when prepared (see above). The percentage of paclitaxel in each fraction (i.e., layer n) was determined using the following equation:

# 4. RESULTS AND DISCUSSION

## *4.1 Creating the Standard Curve for Alkaline Pyrophosphatase*

Before employing the assay on the collected fractions, a "standard curve" of alkaline pyrophosphatase was created with cell samples; this was done to confirm the assay was working as expected in the *Taxus* cell system. This assay was performed on both the lysed living cells and the lyophilized cells to ensure that enzymatic activity was not affected by lyophilization. Lyophilized and living cells had the same results as shown in *Figure 15*. To ensure that the samples were not over-saturated, multiple ratios of cell lysate to PBS were assayed. These ratios are represented as percent dilution on the x-axis in *Figure 16*. At 100%, a mixture containing no PBS and cell lysate was added, and at 0%, no cell lysate was added, only PBS.

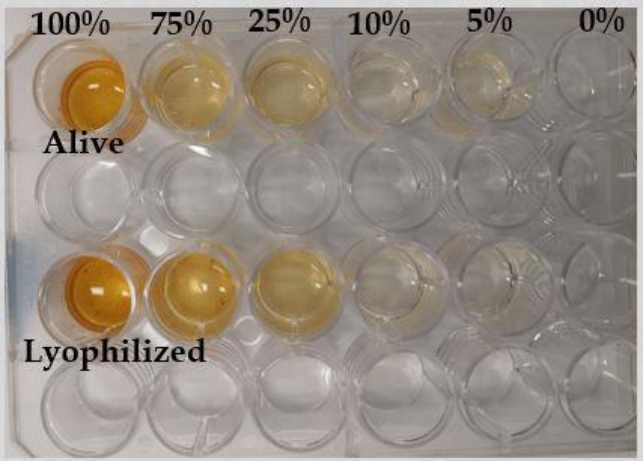


*Figure 15. 24-well plate of alkaline pyrophosphatase activity in lyophilized and lysed living cells. The darker color indicates the presence of alkaline pyrophosphatase*

Through experimental trials, it was determined that the alkaline pyrophosphatase assay took approximately 12 hours of reaction time to generate visible results. It was also noted that the stop solution, trichloroacetic acid, diluted the yellow color, causing a lower absorbance reading. The assays were tested using a plate reader (Fisher Scientific AccuskanGO) at an absorbance range of 405 to 414 nm as shown in *Figure 16*. Because there was no significant difference observed between the absorbances, 405 nm was used for all future assays.

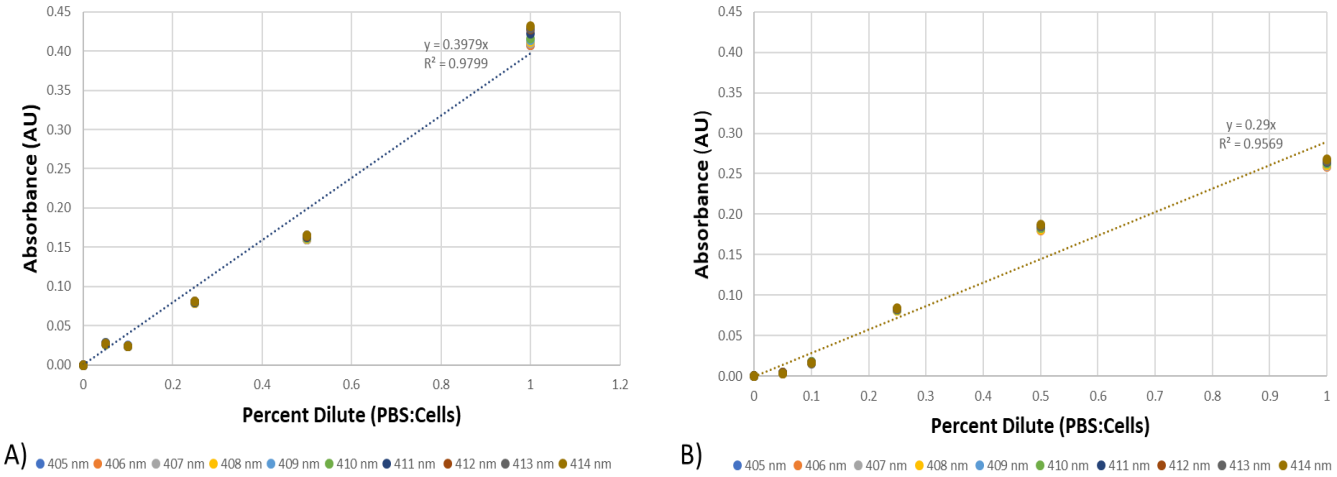


*Figure 16.* A) *Linear curve of different concentrations of lysed living cells in the alkaline pyrophosphatase assay,* B) *Linear curve of different concentrations of lyophilized cells in the alkaline pyrophosphatase assay*

## *4.2 Creating the Standard Curve for Acid Phosphatase*

Before employing the assay on the collected fractions, a "standard curve" of acid phosphatase was created with cell samples; this was done to confirm the assay was working as expected in the *Taxus* cell system. Again, the assay was performed on both living cells and lyophilized cells (both processed with mortar and pestle) to ensure that enzymatic activity was not affected by lyophilization. To ensure that the samples were not over-saturated, a ratio of cell lysate to PBS was added. At 100%, a mixture containing no PBS and cell lysate was added, and at 0%, no cell lysate was added, only PBS. *Figure 17* shows that the lyophilized and alive cells follow a similar trend.

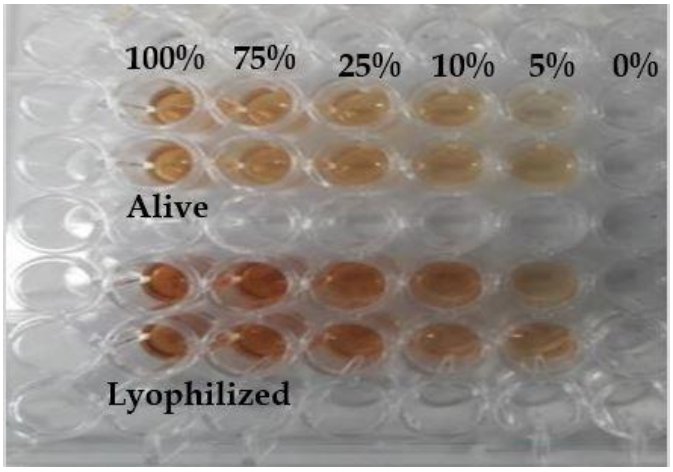


*Figure 17. 96-well plate of acid phosphatase activity in lyophilized and lysed living cells. The darker color indicates the presence of acid phosphatase*

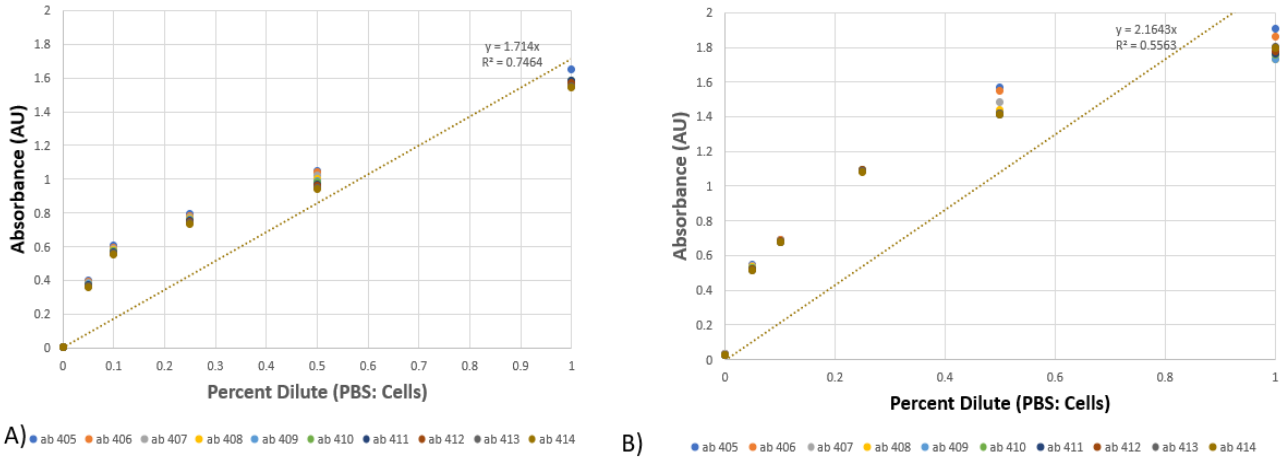


*Figure 18.* A) *Linear curve of different concentrations of lysed living cells in the acid phosphatase assay,* B) *Linear curve of different concentrations of lyophilized cells in the acid phosphatase assay*

Statistical analysis was performed on the linear trend line for each graph; the $R^2$ value for lysed living cells was 0.75, while the $R^2$ value for lyophilized cells was 0.56. Linear regression statistical analysis was performed to ensure the linearity of the line to ensure that the line did not reach a horizontal asymptote. Typically, with enzymatic assays, if the solution is over-saturated, the absorbance readings will plateau and reach a horizontal asymptote as concentration is increased, as shown above in *Figure 18*. As shown in *Figure 18,* there were two linear portions of the graph,

between 0 to 0.2 and 0.5 to 1. However, because absorbance readings lower than 0.600 AU was unfavorable (based on literature studies), a second curve was generated with concentrations between 0 to 20% of cell lysate to determine if a more linear line could be achieved. This more linear region is observed in *Figure 19*. An $R^2$ value of 0.98 was achieved with a linear fit and there is no longer a "non-linear curve" that. Hence, the acid phosphatase assay showed to be compatible with our cell system. In addition, enzyme activity was not adversely affected upon lyophilization. The raw data can be seen in *Appendix A*.

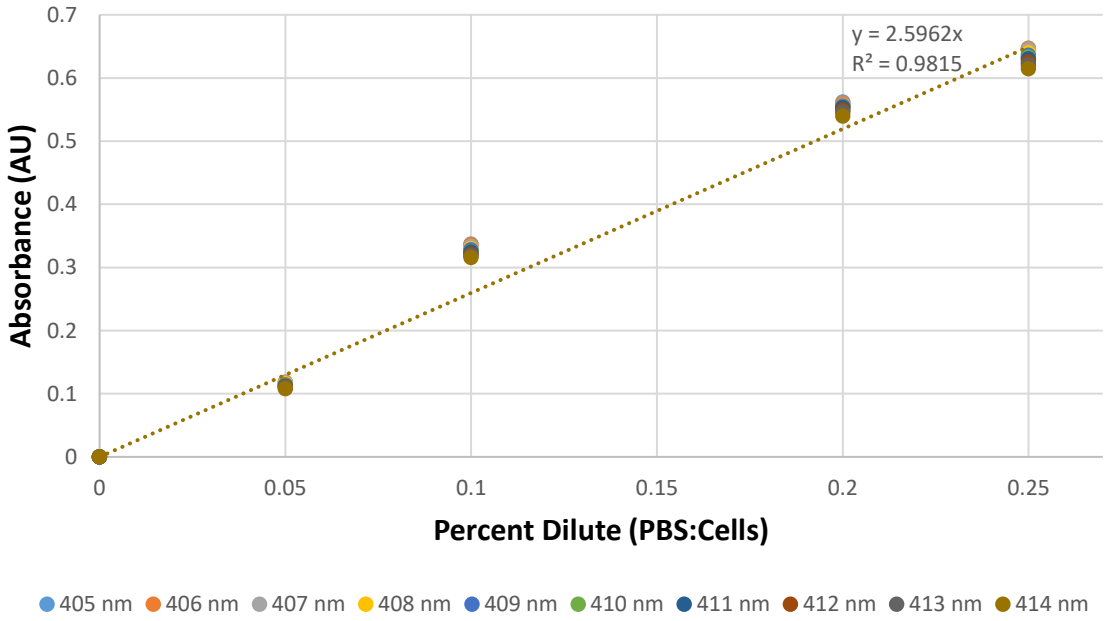


*Figure 19. Standard curve of acid phosphatase activity in different concentrations of lyophilized cells*

## *4.3 Cellular Fractionation Method Development*

The first sucrose gradient tested contained a bottom layer of 1.6 g/mL and a top layer of 1.2 g/mL. The results from the two assays are shown in *Figure 20.* To standardize each experiment for comparison across experiments, the distributions within each layer were calculated using the following formula:

$$\frac{\boldsymbol{Absorbance\ in\ layer\ n}}{\sum(\boldsymbol{Absorbance\ readings})} = \boldsymbol{percentage\ in\ layer\ n}$$

Recall, that the plastid concentration was expected to decrease with increasing sucrose density (due to the low density of plastids) and hence alkaline pyrophosphatase activity was hypothesized to also decrease with increasing sucrose density. The opposite trend was expected for acid phosphatase activity. The raw can be found in *Appendix B.*

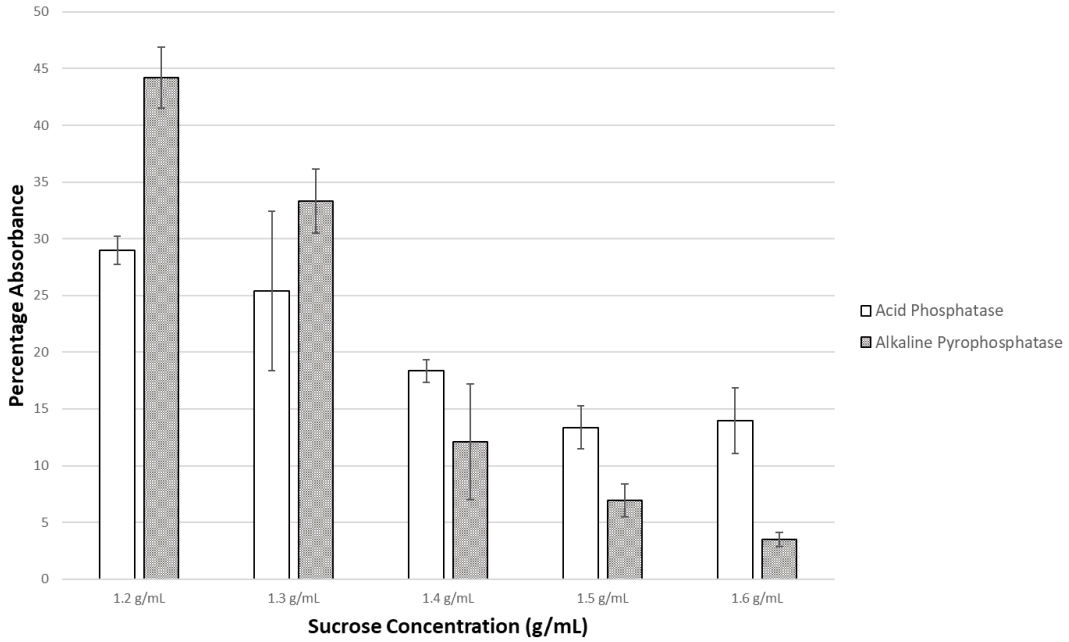


*Figure 20. Distribution of acid pyrophosphatase and alkaline phosphatase in a sucrose gradient (1.2-1.6 g/mL)*

From *Figure 20* both the alkaline pyrophosphatase and acid phosphatase have a similar distribution in the gradient. Because acid phosphatase is the enzyme found in the vacuole, it was expected that the distribution would trend in the opposite direction. It was noted that the concentration of the alkaline pyrophosphatase was consistently high at the lower concentrations with over 40% remaining in the top layer. Based on these results, we decreased the concentrations used in the

sucrose gradient. The sucrose concentration was altered to 0.2 g/mL to 1.0 g/mL and 0.7 g/mL to 1.1 g/mL; results are shown in *Figure 21*.

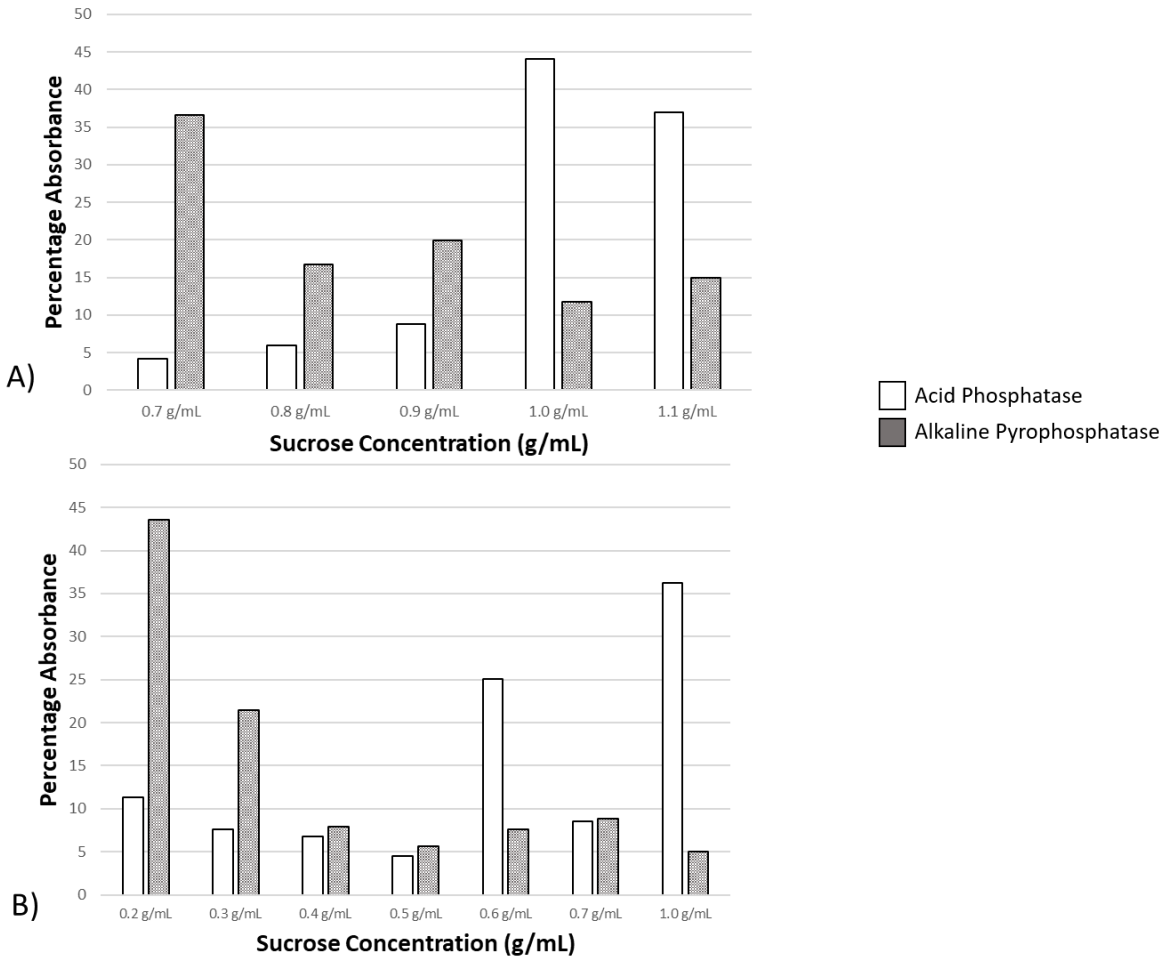


*Figure 21. A) Distribution of acid phosphatase and alkaline pyrophosphatase using sucrose concentrations ranging from 0.7g/mL to 1.1 g/mL. B) Distribution of acid phosphatase and alkaline pyrophosphatase using sucrose concentrations from 0.2 g/mL to 1.0 g/mL*

The results for both gradients showed a clearer separation of the two enzymes tested with the hypothesized distribution observed. The alkaline pyrophosphatase is more concentrated in the less dense layers of sucrose and the distribution decreases as the density increases. Nearly 45% of the enzyme was present in the 0.2 g/mL sucrose and less than 5% was found in the densest layer of 1.0 g/mL (*Figure 21B*). For alkaline pyrophosphatase, over 35% of the enzyme was found to be in

the densest layer of 1.0 g/mL, while only 10% was found in the least dense layer of 0.2 g/mL (*Figure 21B*). Similar trends were observed in *Figure 21A*. These results support the hypothesis that the plastids would be found in the least dense layers and the vacuoles would be found in the densest layers. *Figure 21* demonstrates the feasibility of cell fractionation for *Taxus* plant suspension cultures, which is critical for the proposed localization studies. Density ranges from 0.2g/mL to 1.0g/mL showed a better separation because there was a broader range which allows for better separation, while the 1.0g/mL to 1.6g/mL may not have accounted for lighter organelles. Based on these results, it was decided that the sucrose gradients for all future experiments will be 0.3, 0.5, 0.7, 0.9, 1.1 g/mL.

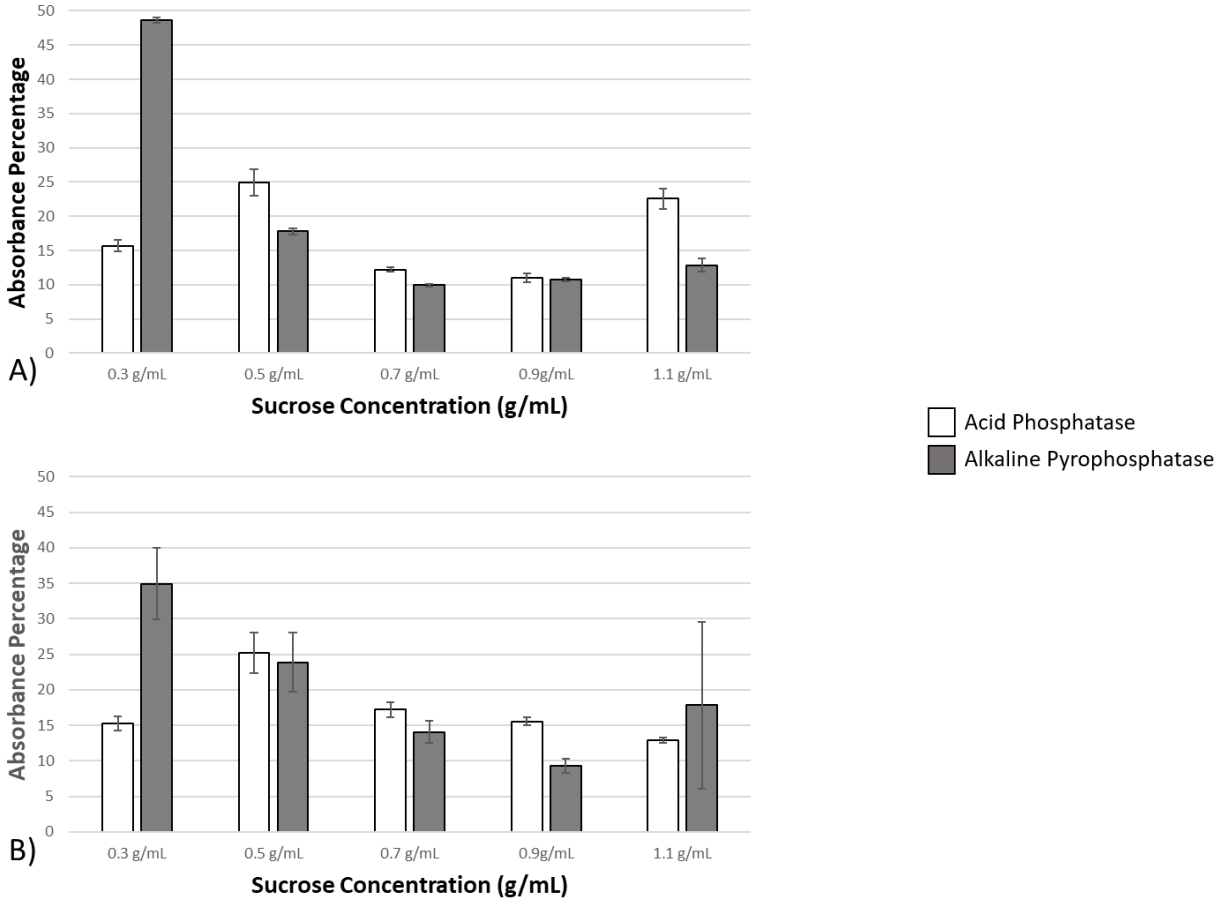


*Figure 22. A) Distribution of acid phosphatase and alkaline pyrophosphatase in day 15 elicited cells. B) Distribution of acid phosphatase and alkaline pyrophosphatase in day 22 elicited cells*

*Figure 22A* shows the experimental results using cells that were elicited with methyl jasmonate on day 7 and sampled on either day 15 (8 days post-elicitation) or day 22 (15 days post-elicitation). We conducted these studies to increase paclitaxel concentration in all samples to minimize difficulties with assay sensitivity. From *Figure 22A*, the concentration of alkaline pyrophosphatase is higher in the least dense sucrose fraction and lower as the density increases. Because alkaline pyrophosphatase is present in plastids, these results suggest that the plastids are most present in the lower density sucrose fractions. *Figure 22B* depicts cells on day 22 (15 days post-elicitation) that were fractionated. While the trend is similar to the day 15 results, there were difficulties with keeping the cell lysate fractionated in the older cell population. After removing samples from the ultracentrifuge, cellular components were clearly fractionated, floating in each distinct fraction. Originally, the layers could settle to ensure clear separation between density gradients (as shown in *Appendix C*). However, after settling on ice for approximately 2 hours, the cell lysate settled at the bottom of the tube. This yielded unusual results because there was not a clear differentiation between the two assays. Further trials would need to be completed with day 22 elicited cells with an adjusted settling time after removing the tubes from the ultracentrifuge.

## *4.4 Methanol Extraction Method Development*

All samples were processed using methods adapted from the methanol extraction process developed in the Roberts lab to quantify paclitaxel in cell culture samples. When the samples were processed using the revised protocol (Section 3.7), the samples crystallized in the evaporative centrifuge. Because of the high concentration of sucrose in the cell fractions, the sucrose was hardened into a solid pellet. Once methanol was added, the sample remained crystallized, making the extraction of paclitaxel from the samples challenging. The samples were broken up manually using a spatula, vortexed, centrifuged, and vigorously shaken to break up the thick sucrose. After

the sucrose had been broken up and mixed with the methanol, the samples were prepared for UPLC analysis as described in Section 3.7. To obtain better results and a higher yield of paclitaxel from the fraction, this procedure could be replicated in 0.5 mL aliquots instead. This will allow for greater extraction of paclitaxel into the methanol, as it will be more manageable to disrupt the sucrose at a smaller volume.

### *4.5 UPLC Results*

Due to laboratory equipment complications, the samples were unable to be run on the UPLC. Based on the UPLC protocol proposed, it was expected that 10-deacetylbaccatin III would elute at approximately 1.0 minutes, baccatin III would elute at approximately 1.9 minutes, and paclitaxel would elute at approximately 3.3 minutes. It is expected that the lower density fractions will show greater peaks in the UPLC data at the 1.0, 1.9 and 3.3-minute marks than in the densest fractions, as paclitaxel is hypothesized to be localized to the plastid fraction. *Figure 23* shows the expected distribution of paclitaxel in the sucrose gradient. Future experiments can be directed towards further resolving paclitaxel localization through the study of additional organelle fractions.

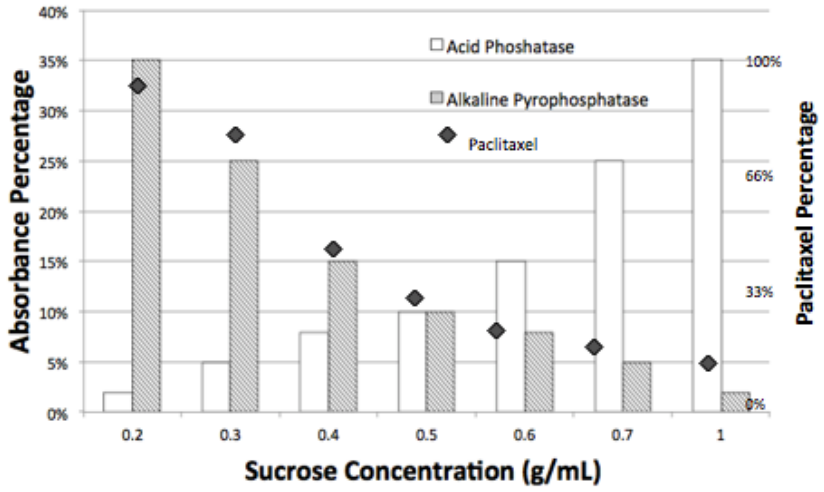


*Figure 23. Expected results of paclitaxel localization in a sucrose gradient*

# 5. CONCLUSION

The methods developed here can be used to identify paclitaxel and precursor location in *Taxus* plant cells. We successfully adapted the alkaline phosphatase and acid pyrophosphatase assays to identify the plastid and vacuole fractions, respectively. A procedure for creating a sucrose gradient for cellular fractionation was developed using ultracentrifugation, and methods for the extraction of hydrophobic compounds (e.g., paclitaxel) from these fractions were optimized. With these methods in place, the intracellular distribution of paclitaxel and related precursors can be determined, and engineering strategies designed to enhance secretion of paclitaxel to the extracellular space.

# 6. FUTURE RECOMMENDATIONS

Future experiments should include assaying the cellular fractions using phosphofructokinase to indicate which fractions contain cytosolic cell components, which literature has suggested has a density between that of plastids and vacuoles (31). This would be beneficial data to include, since literature suggests that paclitaxel is more abundant in the cytosol than plastid. If this were found to be true, the production and extraction of paclitaxel would be targeted to towards these main two organelles.

# 7. REFERENCES


1. Alberts B JA, Lewis J, et al. Molecular Biology of the Cell: Fractionation of Cells. 4th ed. New York: Garland Science 2003.
2. Kishiko Okada ST, Masaya Shiraishi Electron Microscopic Obeservation of Plastid Containing Taxol-like Substances in Callus Cells of *Taxus cuspidata* var. Nana. Pakistan Journal of Biological Sciences 2004:2139-48.
3. Chemler JA, Yan Y, Koffas MAG. Biosynthesis of isoprenoids, polyunsaturated fatty acids and flavonoids in Saccharomyces cerevisiae. Microbial Cell Factories. 2006;5:20-.
4. Magdalena Dzialo JM, Urszula Korzun, Marta Preisner, Jan Szopa, Anna Kulma. The Potential of Plant Phenolics in Prevention and Therapy of Skin Disorders. International Journal of Molecular Sciences 2016.
5. You PSF. What is an Alkaloid? Classification of Alkaloids Plant Science for You [Available from:http://www.plantscience4u.com/2013/02/what-is-alkaloid.html#.WpfSu-gbM2x.
6. Howat S, Park B, Oh IS, Jin YW, Lee EK, Loake GJ. Paclitaxel: biosynthesis, production and future prospects. New biotechnology. 2014;31(3):242-5.
7. NCBI. Paclitaxel: NCBI
8. S. Rao LH, S. Chakravarty, I. Ojima, G.A. Orr, S.B. Horwitz. Characterization of the Taxol Binding Site on the Microtubule. Identification of Arg282 in b-tubulin as the Site of Photoincorporation of a 7-Benzophenone Analogue of Taxol. J Biol Chem 1999.
9. Paclitaxel History [Internet]. News Medical 2014 [cited May 23, 2017]. Available from: https://www.news-medical.net/health/Paclitaxel-History.aspx.
10. Society AC. Discovery of Camptothecin and Taxol [Available from: http://www.acs.org/content/acs/en/education/whatischemistry/landmarks/camptothecintaxol.html .
11. Health USNIo. Success Story: Taxol National Cancer Institute 2005 [Available from: https://dtp.cancer.gov/timeline/flash/success_stories/s2_taxol.htm.
12. Roberts SC. Production and engineering of terpenoids in plant cell culture. Nature chemical biology. 2007;3(7):387-95.
13. Zocher R, Weckwerth W, Hacker C, Kammer B, Hornbogen T, Ewald D. Biosynthesis of Taxol: Enzymatic Acetylation of 10-Deacetylbaccatin-III to Baccatin-III in Crude Extracts from Roots ofTaxus baccata. Biochemical and Biophysical Research Communications. 1996;229(1):16-20.
14. Baloglu E. A New Synthesis of Taxol from Baccatin III Virginia Virginia Polytechnic Institute 1998.
15. Charles Bolsinger AJ. Northeastern Area: State and Private Forestry 2017 [
16. Nicolaou KC, Nantermet PG, Ueno H, Guy RK, Couladouros EA, Sorensen EJ. Total Synthesis of Taxol. 1. Retrosynthesis, Degradation, and Reconstitution. Journal of the American Chemical Society. 1995;117(2):624-33.
17. Crown J, O'Leary M. The taxanes: an update. Lancet (London, England). 2000;355(9210):1176-8.
18. Engels B, Dahm P, Jennewein S. Metabolic engineering of taxadiene biosynthesis in yeast as a first step towards Taxol (Paclitaxel) production. Metabolic engineering. 2008;10(3-4):201-6.
19. Williams DC, Wildung MR, Jin AQ, Dalal D, Oliver JS, Coates RM, et al. Heterologous expression and characterization of a "Pseudomature" form of taxadiene synthase involved in paclitaxel (Taxol) biosynthesis and evaluation of a potential intermediate and inhibitors of the

multistep diterpene cyclization reaction. Archives of biochemistry and biophysics. 2000;379(1):137-46.
20. Book H. Plant Tissue Culture Media 2011 [Available from: https://www.hourlybook.com/plant-tissue-culture-media/.
21. Yukimune Y, Tabata H, Higashi Y, Hara Y. Methyl jasmonate-induced overproduction of paclitaxel and baccatin III in Taxus cell suspension cultures. Nature biotechnology. 1996;14(9):1129-32.
22. Naill MC, Kolewe ME, Roberts SC. Paclitaxel uptake and transport in Taxus cell suspension cultures. Biochemical engineering journal. 2012;63:50-6.
23. Frense D. Taxanes: perspectives for biotechnological production. Applied microbiology and biotechnology. 2007;73(6):1233-40.
24. Naill MC, Kolewe ME, Roberts SC. Paclitaxel uptake and transport in Taxus cell suspension cultures. Biochemical engineering journal. 2012;63:50-6.
25. Russin WA, Ellis DD, Gottwald JR, Zeldin EL, Brodhagen M, Evert RF. Immunocytochemical Localization of Taxol in Taxus cuspidata. International Journal of Plant Sciences. 1995;156(5):668-78.
26. Choi HK, Kim SI, Song JY, Son JS, Hong SS, Durzan D, et al. Localization of paclitaxel in suspension culture of Taxus chinensis2001. 458-62 p.
27. Krueger S, Steinhauser D, Lisec J, Giavalisco P. Analysis of subcellular metabolite distributions within Arabidopsis thaliana leaf tissue: a primer for subcellular metabolomics. Methods in molecular biology (Clifton, NJ). 2014;1062:575-96.
28. Fürtauer L, Weckwerth W, Nägele T. A Benchtop Fractionation Procedure for Subcellular Analysis of the Plant Metabolome. Frontiers in Plant Science. 2016;7:1912.
29. Cox RP, Gilbert P, Jr., Griffin MJ. Alkaline inorganic pyrophosphatase activity of mammalian-cell alkaline phosphatase. The Biochemical journal. 1967;105(1):155-61.
30. Jelitto T, Sonnewald U, Willmitzer L, Hajirezeai M, Stitt M. Inorganic pyrophosphate content and metabolites in potato and tobacco plants expressing E. coli pyrophosphatase in their cytosol. Planta. 1992;188(2):238-44.
31. Hausler RE, Holtum JA, Latzko E. Cytosolic ATP-Dependent Phosphofructokinase from Spinach. Plant physiology. 1987;84(2):205-7.

# 8. APPENDIX

## *Appendix A: Raw Data of Creating a Standard Curve for Enzymatic Assays*

Alkaline Pyrophosphatase

| 405nm | | | | | | |
|---|---|---|---|---|---|---|
| Dilution | 1 | 0.5 | 0.25 | 0.1 | 0.05 | 0 |
| Absorbance | 0.334 | 0.1705 | 0.081 | 0.021 | 0.016 | 0 |
| 406 nm | | | | | | |
| Dilution | 1 | 0.5 | 0.25 | 0.1 | 0.05 | 0 |
| Absorbance | 0.3335 | 0.17 | 0.0805 | 0.0205 | 0.0155 | 0 |
| 407nm | | | | | | |
| Dilution | 1 | 0.5 | 0.25 | 0.1 | 0.05 | 0 |
| Absorbance | 0.335 | 0.1705 | 0.0805 | 0.02 | 0.0155 | 0 |
| 408 nm | | | | | | |
| Dilution | 1 | 0.5 | 0.25 | 0.1 | 0.05 | 0 |
| Absorbance | 0.3365 | 0.171 | 0.08 | 0.02 | 0.015 | 0 |
| 409 nm | | | | | | |
| Dilution | 1 | 0.5 | 0.25 | 0.1 | 0.05 | 0 |
| Absorbance | 0.3385 | 0.1725 | 0.081 | 0.0205 | 0.016 | 0 |
| 410 nm | | | | | | |
| Dilution | 1 | 0.5 | 0.25 | 0.1 | 0.05 | 0 |
| Absorbance | 0.3395 | 0.173 | 0.0815 | 0.0205 | 0.015 | 0 |
| 411nm | | | | | | |
| Dilution | 1 | 0.5 | 0.25 | 0.1 | 0.05 | 0 |
| Absorbance | 0.3435 | 0.174 | 0.0815 | 0.02 | 0.0155 | 0 |
| 412 nm | | | | | | |
| Dilution | 1 | 0.5 | 0.25 | 0.1 | 0.05 | 0 |
| Absorbance | 0.347 | 0.1745 | 0.082 | 0.02 | 0.0155 | 0 |
| 413nm | | | | | | |
| Dilution | 1 | 0.5 | 0.25 | 0.1 | 0.05 | 0 |
| Absorbance | 0.3475 | 0.175 | 0.082 | 0.0195 | 0.0155 | 0 |
| 414 nm | | | | | | |
| Dilution | 1 | 0.5 | 0.25 | 0.1 | 0.05 | 0 |
| Absorbance | 0.35 | 0.176 | 0.0825 | 0.02 | 0.015 | 0 |

Acid Test I

| Absorbance 405 | | | | | | |
|---|---|---|---|---|---|---|
| Alive (avg) | 1.655 | 1.05 | 0.792 | 0.6045 | 0.3975 | 0.008 |
| Dead (avg) | 1.907 | 1.566 | 1.085 | 0.689 | 0.55 | 0.034 |
| Dilution | 1 | 0.5 | 0.25 | 0.1 | 0.05 | 0 |
| Absorbance 406 | | | | | | |
| Alive (avg) | 1.56 | 1.04 | 0.783 | 0.5945 | 0.391 | 0.007 |
| Dead (avg) | 1.859 | 1.548 | 1.089 | 0.689 | 0.544 | 0.033 |
| Dilution | 1 | 0.5 | 0.25 | 0.1 | 0.05 | 0 |
| Absorbance 407 | | | | | | |
| Alive (avg) | 1.556 | 1.023 | 0.776 | 0.589 | 0.388 | 0.007 |
| Dead (avg) | 1.757 | 1.484 | 1.092 | 0.682 | 0.538 | 0.033 |
| Dilution | 1 | 0.5 | 0.25 | 0.1 | 0.05 | 0 |
| Absorbance 408 | | | | | | |
| Alive (avg) | 1.558 | 1.002 | 0.768 | 0.581 | 0.383 | 0.005 |
| Dead (avg) | 1.733 | 1.441 | 1.086 | 0.679 | 0.532 | 0.03 |
| Dilution | 1 | 0.5 | 0.25 | 0.1 | 0.05 | 0 |
| Absorbance 409 | | | | | | |
| Alive (avg) | 1.577 | 0.99 | 0.763 | 0.577 | 0.379 | 0.005 |
| Dead (avg) | 1.735 | 1.42 | 1.09 | 0.682 | 0.53 | 0.03 |
| Dilution | 1 | 0.5 | 0.25 | 0.1 | 0.05 | 0 |
| Absorbance 410 | | | | | | |
| Alive (avg) | 1.586 | 0.981 | 0.758 | 0.573 | 0.376 | 0.005 |
| Dead (avg) | 1.755 | 1.417 | 1.091 | 0.681 | 0.527 | 0.03 |
| Dilution | 1 | 0.5 | 0.25 | 0.1 | 0.05 | 0 |
| Absorbance 411 | | | | | | |
| Alive (avg) | 1.583 | 0.972 | 0.752 | 0.567 | 0.372 | 0.004 |
| Dead (avg) | 1.763 | 1.411 | 1.09 | 0.68 | 0.522 | 0.03 |
| Dilution | 1 | 0.5 | 0.25 | 0.1 | 0.05 | 0 |
| Absorbance 412 | | | | | | |
| Alive (avg) | 1.569 | 0.961 | 0.748 | 0.563 | 0.369 | 0.004 |
| Dead (avg) | 1.78 | 1.42 | 1.093 | 0.681 | 0.52 | 0.029 |
| Dilution | 1 | 0.5 | 0.25 | 0.1 | 0.05 | 0 |
| Absorbance 413 | | | | | | |
| Alive (avg) | 1.552 | 0.952 | 0.742 | 0.558 | 0.365 | 0.003 |
| Dead (avg) | 1.801 | 1.418 | 1.089 | 0.679 | 0.515 | 0.029 |
| Dilution | 1 | 0.5 | 0.25 | 0.1 | 0.05 | 0 |
| Absorbance 414 | | | | | | |
| Alive (avg) | 1.542 | 0.943 | 0.737 | 0.552 | 0.361 | 0.003 |
| Dead (avg) | 1.798 | 1.411 | 1.083 | 0.678 | 0.512 | 0.029 |
| Dilution | 1 | 0.5 | 0.25 | 0.1 | 0.05 | 0 |

Acid Test II

| 405nm | | | | | |
|---|---|---|---|---|---|
| Dilution | 0.25 | 0.2 | 0.1 | 0.05 | 0 |
| Absorbance | 0.647 | 0.561667 | 0.336667 | 0.117667 | 0 |
| 406 nm | | | | | |
| Dilution | 0.25 | 0.2 | 0.1 | 0.05 | 0 |
| Absorbance | 0.646333 | 0.56 | 0.336 | 0.117667 | 0 |
| 407nm | | | | | |
| Dilution | 0.25 | 0.2 | 0.1 | 0.05 | 0 |
| Absorbance | 0.644333 | 0.557333 | 0.332667 | 0.116667 | 0 |
| 408 nm | | | | | |
| Dilution | 0.25 | 0.2 | 0.1 | 0.05 | 0 |
| Absorbance | 0.64 | 0.555333 | 0.329667 | 0.115667 | 0 |
| 409 nm | | | | | |
| Dilution | 0.25 | 0.2 | 0.1 | 0.05 | 0 |
| Absorbance | 0.636 | 0.555 | 0.327667 | 0.113667 | 0 |
| 410 nm | | | | | |
| Dilution | 0.25 | 0.2 | 0.1 | 0.05 | 0 |
| Absorbance | 0.632667 | 0.554 | 0.324667 | 0.113 | 0 |
| 411nm | | | | | |
| Dilution | 0.25 | 0.2 | 0.1 | 0.05 | 0 |
| Absorbance | 0.630333 | 0.553 | 0.324 | 0.112 | 0 |
| 412 nm | | | | | |
| Dilution | 0.25 | 0.2 | 0.1 | 0.05 | 0 |
| Absorbance | 0.625333 | 0.549 | 0.320667 | 0.110667 | 0 |
| 413nm | | | | | |
| Dilution | 0.25 | 0.2 | 0.1 | 0.05 | 0 |
| Absorbance | 0.620667 | 0.545333 | 0.318667 | 0.109667 | 0 |
| 414 nm | | | | | |
| Dilution | 0.25 | 0.2 | 0.1 | 0.05 | 0 |
| Absorbance | 0.614667 | 0.539667 | 0.315667 | 0.108 | 0 |

## *Appendix B: Raw Data of Acid Phosphatase and Alkaline Pyrophosphatase Absorbance readings*

Obtained on January 24th, 2018

**DATE: JAN. 24TH**

**ACID ASSAY**

| Absorbance | top layer | 1.2 g/mL | 1.3 g/mL | 1.4 g/mL | 1.5 g/mL | 1.6 g/mL | blank |
|---|---|---|---|---|---|---|---|
| Trial 1 | 0.95 | 0.75 | 0.807 | 0.487 | 0.345 | 0.342 | 0.042 |
| Trial 2 | 0.844 | 0.855 | 0.598 | 0.561 | 0.444 | 0.478 | 0.044 |

**SUBTRACTION OF BLANK**

| Absorbance | top layer | 1.2 g/mL | 1.3 g/mL | 1.4 g/mL | 1.5 g/mL | 1.6 g/mL | blank |
|---|---|---|---|---|---|---|---|
| Trial 1 | 0.908 | 0.708 | 0.765 | 0.445 | 0.303 | 0.3 | 0 |
| Trial 2 | 0.8 | 0.811 | 0.554 | 0.517 | 0.4 | 0.434 | 0 |

**PERCENTAGE ABSORBANCE**

| Absorbance | top layer | 1.2 g/mL | 1.3 g/mL | 1.4 g/mL | 1.5 g/mL | 1.6 g/mL | Total |
|---|---|---|---|---|---|---|---|
| Trial 1 | 26.48002 | 20.64742 | 22.30971 | 12.97754 | 8.836395 | 8.748906 | 3.429 |
| Trial 2 | 22.75313 | 23.06598 | 15.75654 | 14.70421 | 11.37656 | 12.34357 | 3.516 |

**PERCENTAGE ABSORBANCE-NO TOP LAYER**

| Absorbance | 1.2 g/mL | 1.3 g/mL | 1.4 g/mL | 1.5 g/mL | 1.6 g/mL | Total |
|---|---|---|---|---|---|---|
| Trial 1 | 28.08409 | 30.3451 | 17.65173 | 12.01904 | 11.90004 | 2.521 |
| Trial 2 | 29.86009 | 20.39764 | 19.03535 | 14.72754 | 15.97938 | 2.716 |
| std | 1.255818 | 7.033915 | 0.978368 | 1.915199 | 2.88453 | |

**ALKALINE ASSAY**

| Absorbance | top layer | 1.2 g/mL | 1.3 g/mL | 1.4 g/mL | 1.5 g/mL | 1.6 g/mL | blank |
|---|---|---|---|---|---|---|---|
| Trial 1 | 0.452 | 0.291 | 0.218 | 0.148 | 0.078 | 0.064 | 0.044 |
| Trial 2 | 0.434 | 0.295 | 0.228 | 0.094 | 0.08 | 0.062 | 0.047 |
| Trial 3 | 0.367 | 0.312 | 0.266 | 0.103 | 0.098 | 0.07 | 0.044 |

**SUBTRACTION OF BLANK**

| Absorbance | top layer | 1.2 g/mL | 1.3 g/mL | 1.4 g/mL | 1.5 g/mL | 1.6 g/mL | blank |
|---|---|---|---|---|---|---|---|
| Trial 1 | 0.408 | 0.247 | 0.174 | 0.104 | 0.034 | 0.02 | 0 |
| Trial 2 | 0.387 | 0.248 | 0.181 | 0.047 | 0.033 | 0.015 | 0 |
| Trial 3 | 0.323 | 0.268 | 0.222 | 0.059 | 0.054 | 0.026 | 0 |

**PERCENTAGE ABSORBANCE**

| Absorbance | top layer | 1.2 g/mL | 1.3 g/mL | 1.4 g/mL | 1.5 g/mL | 1.6 g/mL | Total |
|---|---|---|---|---|---|---|---|
| Trial 1 | 41.33739 | 25.02533 | 17.62918 | 10.53698 | 3.444782 | 2.026342 | 0.987 |
| Trial 2 | 42.48079 | 27.22283 | 19.86828 | 5.159166 | 3.622393 | 1.646542 | 0.911 |
| Trial 3 | 33.92857 | 28.15126 | 23.31933 | 6.197479 | 5.672269 | 2.731092 | 0.952 |
| Average | 39.24892 | 26.79981 | 20.27226 | 7.297875 | 4.246481 | 2.134659 | |

**PERCENTAGE ABSORBANCE-NO TOP LAYER**

| Absorbance | 1.2 g/mL | 1.3 g/mL | 1.4 g/mL | 1.5 g/mL | 1.6 g/mL | Total |
|---|---|---|---|---|---|---|
| Trial 1 | 42.65976 | 30.05181 | 17.962 | 5.872193 | 3.454231 | 0.579 |
| Trial 2 | 47.32824 | 34.54198 | 8.969466 | 6.29771 | 2.862595 | 0.524 |
| Trial 3 | 42.60731 | 35.29412 | 9.379968 | 8.585056 | 4.133545 | 0.629 |
| Average | 44.19844 | 33.29597 | 12.10381 | 6.91832 | 3.483457 | |
| std | 2.710618 | 2.834581 | 5.077492 | 1.459031 | 0.635979 | |

Obtained on January 26th, 2018

**DATE: JAN. 26TH**

**ACID ASSAY**

| Absorbance | 0.8 g/mL | 0.9 g/mL | 1.0 g/mL | 1.1 g/mL | 1.2 g/mL | Blank |
|---|---|---|---|---|---|---|
| Trial 1 | 1.348 | 1.398 | 0.384 | 0.279 | 0.236 | 0.043 |
| | | | | | | |
| Absorbance | 0.7 g/mL | 0.8 g/mL | 0.9 g/mL | 1.0 g/mL | 1.1 g/mL | Blank |
| Trial 2 | 1.325 | 0.801 | 0.615 | 0.389 | 0.252 | 0.046 |

**SUBTRACTION OF BLANK**

| Absorbance | 0.8 g/mL | 0.9 g/mL | 1.0 g/mL | 1.1 g/mL | 1.2 g/mL | Blank |
|---|---|---|---|---|---|---|
| Trial 1 | 1.305 | 1.355 | 0.341 | 0.236 | 0.193 | 0 |
| | | | | | | |
| Absorbance | 0.7 g/mL | 0.8 g/mL | 0.9 g/mL | 1.0 g/mL | 1.1 g/mL | Blank |
| Trial 2 | 1.279 | 0.755 | 0.569 | 0.343 | 0.206 | 0 |

**PERCENTAGE ABSORBANCE**

| Absorbance | 0.8 g/mL | 0.9 g/mL | 1.0 g/mL | 1.1 g/mL | 1.2 g/mL | total |
|---|---|---|---|---|---|---|
| Trial 1 | 38.0466472 | 39.50437 | 9.941691 | 6.880466 | 5.626822 | 3.43 |
| | | | | | | |
| Absorbance | 0.7 g/mL | 0.8 g/mL | 0.9 g/mL | 1.0 g/mL | 1.1 g/mL | total |
| Trial 2 | 40.5774112 | 23.95305 | 18.05203 | 10.88198 | 6.535533 | 3.152 |

**ALKALINE ASSAY**

| Absorbance | 0.8 g/mL | 0.9 g/mL | 1.0 g/mL | 1.1 g/mL | 1.2 g/mL | Blank |
|---|---|---|---|---|---|---|
| Trial 1 | 0.529 | 0.304 | 0.11 | 0.068 | 0.076 | 0.044 |
| | | | | | | |
| Absorbance | 0.7 g/mL | 0.8 g/mL | 0.9 g/mL | 1.0 g/mL | 1.1 g/mL | Blank |
| Trial 2 | 0.332 | 0.182 | 0.135 | 0.067 | 0.069 | 0.047 |

**SUBTRACTION OF BLANK**

| Absorbance | 0.8 g/mL | 0.9 g/mL | 1.0 g/mL | 1.1 g/mL | 1.2 g/mL | Blank |
|---|---|---|---|---|---|---|
| Trial 1 | 0.485 | 0.26 | 0.066 | 0.024 | 0.032 | 0 |
| | | | | | | |
| Absorbance | 0.7 g/mL | 0.8 g/mL | 0.9 g/mL | 1.0 g/mL | 1.1 g/mL | Blank |
| Trial 2 | 0.285 | 0.135 | 0.088 | 0.02 | 0.022 | 0 |

**PERCENTAGE ABSORBANCE**

| Absorbance | 0.8 g/mL | 0.9 g/mL | 1.0 g/mL | 1.1 g/mL | 1.2 g/mL | total |
|---|---|---|---|---|---|---|
| Trial 1 | 55.9400231 | 29.988466 | 7.61245675 | 2.76816609 | 3.69088812 | 0.867 |
| | | | | | | |
| Absorbance | 0.7 g/mL | 0.8 g/mL | 0.9 g/mL | 1.0 g/mL | 1.1 g/mL | total |
| Trial 2 | 51.8181818 | 24.5454545 | 16 | 3.63636364 | 4 | 0.55 |

## Obtained on January 30th, 2018

**DATE: JAN. 30TH**

**ACID ASSAY**

| Absorbanc | top | top layer | 0.2 g/mL | 0.3 g/mL | 0.4 g/mL | 0.5 g/mL | 0.6 g/mL | 0.7 g/mL | 1.0 g/mL | blank |
|---|---|---|---|---|---|---|---|---|---|---|
| Trial 1 | 2.079 | 1.709 | 0.753 | 0.517 | 0.47 | 0.326 | 1.617 | 0.578 | 2.317 | 0.043 |
| | | | | | | | | | | |
| Absorbanc | Top layer | Top | 0.7 g/mL | 0.8 g/mL | 0.9 g/mL | 1.0 g/mL | 1.1 g/mL | Blank | | |
| Trial 2 | 2.371 | 0.26 | 0.224 | 0.3 | 0.42 | 1.925 | 1.622 | 0.045 | | |

**SUBTRACTION OF BLANK**

| Absorbanc | top | top layer | 0.2 g/mL | 0.3 g/mL | 0.4 g/mL | 0.5 g/mL | 0.6 g/mL | 0.7 g/mL | 1.0 g/mL | blank |
|---|---|---|---|---|---|---|---|---|---|---|
| Trial 1 | 2.036 | 1.666 | 0.71 | 0.474 | 0.427 | 0.283 | 1.574 | 0.535 | 2.274 | 0 |
| | | | | | | | | | | |
| Absorbanc | Top layer | Top | 0.7 g/mL | 0.8 g/mL | 0.9 g/mL | 1.0 g/mL | 1.1 g/mL | Blank | | |
| Trial 2 | 2.326 | 0.215 | 0.179 | 0.255 | 0.375 | 1.88 | 1.577 | 0 | | |

**PERCENTAGE ABSORBANCE**

| Absorbanc | top | top layer | 0.2 g/mL | 0.3 g/mL | 0.4 g/mL | 0.5 g/mL | 0.6 g/mL | 0.7 g/mL | 1.0 g/mL | total |
|---|---|---|---|---|---|---|---|---|---|---|
| Trial 1 | 20.402846 | 16.69506 | 7.114941 | 4.749975 | 4.2789859 | 2.835956 | 15.77312 | 5.361259 | 22.78785 | 9.979 |
| | | | | | | | | | | |
| e | (PBS) | Layer | 0.7 g/mL | 0.8 g/mL | 0.9 g/mL | 1.0 g/mL | 1.1 g/mL | | | total |
| Trial 2 | 34.1707066 | 3.158513 | 2.629646 | 3.746144 | 5.5090348 | 27.61863 | 23.16733 | | | 6.807 |

**PERCENTAGE ABSORBANCE-NO TOP LAYER**

| Absorbanc | 0.2 g/mL | 0.3 g/mL | 0.4 g/mL | 0.5 g/mL | 0.6 g/mL | 0.7 g/mL | 1.0 g/mL | total |
|---|---|---|---|---|---|---|---|---|
| Trial 1 | 11.3111359 | 7.551378 | 6.802613 | 4.508523 | 25.075673 | 8.52318 | 36.2275 | 6.277 |
| | | | | | | | | |
| Absorbanc | 0.7 g/mL | 0.8 g/mL | 0.9 g/mL | 1.0 g/mL | 1.1 g/mL | | | total |
| Trial 2 | 4.19596812 | 5.977496 | 8.790436 | 44.06939 | 36.966714 | | | 4.266 |

**ALKALINE ASSAY**

| Absorbance | top | top layer | 0.2 g/mL | 0.3 g/mL | 0.4 g/mL | 0.5 g/mL | 0.6 g/mL | 0.7 g/mL | 1.0 g/mL | blank |
|---|---|---|---|---|---|---|---|---|---|---|
| Trial 1 | 0.181 | 0.569 | 0.184 | 0.114 | 0.071 | 0.064 | 0.07 | 0.074 | 0.062 | 0.046 |
| | | | | | | | | | | |
| Absorbance | Top layer | Top Layer | 0.7 g/mL | 0.8 g/mL | 0.9 g/mL | 1.0 g/mL | 1.1 g/mL | Blank | | |
| Trial 2 | 0.272 | 0.165 | 0.107 | 0.075 | 0.08 | 0.067 | 0.072 | 0.048 | | |

**SUBTRACTION OF BLANK**

| Absorbance | top | top layer | 0.2 g/mL | 0.3 g/mL | 0.4 g/mL | 0.5 g/mL | 0.6 g/mL | 0.7 g/mL | 1.0 g/mL | blank |
|---|---|---|---|---|---|---|---|---|---|---|
| Trial 1 | 0.135 | 0.523 | 0.138 | 0.068 | 0.025 | 0.018 | 0.024 | 0.028 | 0.016 | 0 |
| | | | | | | | | | | |
| Absorbance | Top layer | Top Layer | 0.7 g/mL | 0.8 g/mL | 0.9 g/mL | 1.0 g/mL | 1.1 g/mL | Blank | | |
| Trial 2 | 0.224 | 0.117 | 0.059 | 0.027 | 0.032 | 0.019 | 0.024 | 0 | | |

**PERCENTAGE ABSORBANCE**

| Absorbance | top | top layer | 0.2 g/mL | 0.3 g/mL | 0.4 g/mL | 0.5 g/mL | 0.6 g/mL | 0.7 g/mL | 1.0 g/mL | total |
|---|---|---|---|---|---|---|---|---|---|---|
| Trial 1 | 13.8461538 | 53.6410256 | 14.1538462 | 6.97435897 | 2.56410256 | 1.84615385 | 2.46153846 | 2.87179487 | 1.64102564 | 0.975 |
| | | | | | | | | | | |
| Absorbance | (PBS) | (PBS) | 0.7 g/mL | 0.8 g/mL | 0.9 g/mL | 1.0 g/mL | 1.1 g/mL | | | total |
| Trial 2 | 44.6215139 | 23.3067729 | 11.752988 | 5.37848606 | 6.37450199 | 3.78486056 | 4.78087649 | | | 0.502 |

**PERCENTAGE ABSORBANCE-NO TOP LAYER**

| Absorbance | 0.2 g/mL | 0.3 g/mL | 0.4 g/mL | 0.5 g/mL | 0.6 g/mL | 0.7 g/mL | 1.0 g/mL | total |
|---|---|---|---|---|---|---|---|---|
| Trial 1 | 43.533123 | 21.4511041 | 7.88643533 | 5.67823344 | 7.57097792 | 8.83280757 | 5.04731861 | 0.317 |
| | | | | | | | | |
| Absorbance | 0.7 g/mL | 0.8 g/mL | 0.9 g/mL | 1.0 g/mL | 1.1 g/mL | | | total |
| Trial 2 | 36.6459627 | 16.7701863 | 19.8757764 | 11.8012422 | 14.9068323 | | | 0.161 |

## Obtained on February 7th, 2018

**DATE: FEB. 7TH**

**ACID ASSAY**

| Absorbance | Top Layer | 0.3 g/mL | 0.5 g/mL | 0.7 g/mL | 0.9 g/mL | 1.1 g/mL | Blank |
|---|---|---|---|---|---|---|---|
| Trial 1 | 3.896 | 3.901 | 3.935 | 3.761 | 3.924 | 6 | 0.046 |
| Trial 2 | 3.844 | 3.929 | 3.987 | 3.721 | 3.836 | 6 | 0.046 |
| Trial 3 | 3.831 | 3.98 | 3.911 | 3.719 | 3.929 | 6 | 0.046 |

**SUBTRACTION OF BLANK**

| Absorbance | Top Layer | 0.3 g/mL | 0.5 g/mL | 0.7 g/mL | 0.9 g/mL | 1.1 g/mL | Blank |
|---|---|---|---|---|---|---|---|
| Trial 1 | 3.85 | 3.855 | 3.889 | 3.715 | 3.878 | 5.954 | 0 |
| Trial 2 | 3.798 | 3.883 | 3.941 | 3.675 | 3.79 | 5.954 | 0 |
| Trial 3 | 3.785 | 3.934 | 3.865 | 3.673 | 3.883 | 5.954 | 0 |

**PERCENT ABSORBANCE**

| Absorbance | Top Layer | 0.3 g/mL | 0.5 g/mL | 0.7 g/mL | 0.9 g/mL | 1.1 g/mL | Total |
|---|---|---|---|---|---|---|---|
| Trial 1 | 15.31363112 | 15.33351895 | 15.46875621 | 14.77665964 | 15.42500298 | 23.68243109 | 25.141 |
| Trial 2 | 15.16712591 | 15.50656923 | 15.73818937 | 14.67593147 | 15.13517831 | 23.77700571 | 25.041 |
| Trial 3 | 15.08328684 | 15.67705428 | 15.40208815 | 14.63696501 | 15.47381844 | 23.72678728 | 25.094 |
| Average | 15.18801463 | 15.50571415 | 15.53634458 | 14.69651871 | 15.34466658 | 23.72874136 | |
| STD | 0.116584199 | 0.171769258 | 0.177952656 | 0.072086913 | 0.183056655 | 0.047317582 | |

**PERCENT ABSORBANCE-NO TOP LAYER**

| Absorbance | 0.3 g/mL | 0.5 g/mL | 0.7 g/mL | 0.9g/mL | 1.1 g/mL | Total |
|---|---|---|---|---|---|---|
| Trial 1 | 18.10624207 | 18.26593396 | 17.44868724 | 18.21426894 | 27.96486778 | 21.291 |
| Trial 2 | 18.27896248 | 18.5519936 | 17.29981641 | 17.84117121 | 28.0280563 | 21.243 |
| Trial 3 | 18.46168286 | 18.13787601 | 17.23684828 | 18.22234736 | 27.94124548 | 21.309 |
| Average | 18.2822958 | 18.31860119 | 17.32845064 | 18.09259584 | 27.97805652 | |
| STD | 0.177743835 | 0.212022925 | 0.108783618 | 0.217777577 | 0.044883033 | |

**ALKALINE ASSAY**

| Absorbance | Top Layer | 0.3 g/mL | 0.5 g/mL | 0.7 g/mL | 0.9 g/mL | 1.1 g/mL | Blank |
|---|---|---|---|---|---|---|---|
| Trial 1 | 2.039 | 0.979 | 0.482 | 0.562 | 0.373 | 0.192 | 0.043 |
| Trial 2 | 2.041 | 0.977 | 0.481 | 0.559 | 0.372 | 0.192 | 0.043 |
| Trial 3 | 2.042 | 0.976 | 0.48 | 0.556 | 0.371 | 0.191 | 0.044 |

**SUBTRACTION OF BLANK**

| Absorbance | Top Layer | 0.3 g/mL | 0.5 g/mL | 0.7 g/mL | 0.9 g/mL | 1.1 g/mL | Blank |
|---|---|---|---|---|---|---|---|
| Trial 1 | 1.996 | 0.936 | 0.439 | 0.519 | 0.33 | 0.149 | 0 |
| Trial 2 | 1.998 | 0.934 | 0.438 | 0.516 | 0.329 | 0.149 | 0 |
| Trial 3 | 1.998 | 0.932 | 0.436 | 0.512 | 0.327 | 0.147 | 0 |

**PERCENT ABSORBANCE**

| Absorbance | Top Layer | 0.3 g/mL | 0.5 g/mL | 0.7 g/mL | 0.9 g/mL | 1.1 g/mL | Total |
|---|---|---|---|---|---|---|---|
| Trial 1 | 45.68551156 | 21.42366674 | 10.04806592 | 11.87914855 | 7.553215839 | 3.410391394 | 4.369 |
| Trial 2 | 45.78368469 | 21.40238313 | 10.03666361 | 11.82401467 | 7.538955087 | 3.414298808 | 4.364 |
| Trial 3 | 45.90992647 | 21.41544118 | 10.01838235 | 11.76470588 | 7.513786765 | 3.377757353 | 4.352 |
| Average | 45.79304091 | 21.41383035 | 10.03437063 | 11.82262303 | 7.53531923 | 3.400815852 | |
| STD | 0.112499632 | 0.01073285 | 0.014974039 | 0.057234023 | 0.019964407 | 0.020064589 | |

**PERCENT ABSORBANCE-NO TOP LAYER**

| Absorbance | 0.3 g/mL | 0.5 g/mL | 0.7 g/mL | 0.9g/mL | 1.1 g/mL | Total |
|---|---|---|---|---|---|---|
| Trial 1 | 39.4437421 | 18.4997893 | 21.8710493 | 13.90644753 | 6.278971766 | 2.373 |
| Trial 2 | 39.47590871 | 18.51225697 | 21.80896027 | 13.90532544 | 6.297548605 | 2.366 |
| Trial 3 | 39.59218352 | 18.52166525 | 21.7502124 | 13.89124894 | 6.24468989 | 2.354 |
| Average | 39.50394477 | 18.51123717 | 21.81007399 | 13.90100731 | 6.273736753 | |
| STD | 0.078091162 | 0.010973575 | 0.060426148 | 0.008469597 | 0.026815387 | |

Obtained on February 9th, 2018

**DATE: FEB. 9TH**

**ACID ASSAY**

| Absorbance | Top Layer | 0.3 g/mL | 0.5 g/mL | 0.7 g/mL | 0.9 g/mL | 1.1 g/mL | Blank |
|---|---|---|---|---|---|---|---|
| Trial 1 | 3.308 | 3.522 | 3.365 | 3.063 | 3.359 | 2.757 | 0.046 |
| Trial 2 | 3.282 | 2.491 | 3.313 | 3.023 | 3.307 | 2.78 | 0.045 |
| Trial 3 | 3.258 | 3.469 | 3.305 | 2.986 | 3.298 | 2.824 | 0.046 |

**SUBTRACTION OF BLANK**

| Absorbance | Top Layer | 0.3 g/mL | 0.5 g/mL | 0.7 g/mL | 0.9 g/mL | 1.1 g/mL | Blank |
|---|---|---|---|---|---|---|---|
| Trial 1 | 3.262 | 3.476 | 3.319 | 3.017 | 3.313 | 2.711 | 0 |
| Trial 2 | 3.237 | 2.446 | 3.268 | 2.978 | 3.262 | 2.735 | 0 |
| Trial 3 | 3.212 | 3.423 | 3.259 | 2.94 | 3.252 | 2.778 | 0 |

**PERCENT ABSORBANCE**

| Absorbance | Top Layer | 0.3 g/mL | 0.5 g/mL | 0.7 g/mL | 0.9 g/mL | 1.1 g/mL | Total |
|---|---|---|---|---|---|---|---|
| Trial 1 | 17.08032255 | 18.20085873 | 17.37878312 | 15.7974657 | 17.34736622 | 14.19520369 | 19.098 |
| Trial 2 | 18.05757001 | 13.64498494 | 18.23050318 | 16.61274127 | 18.19703224 | 15.25716836 | 17.926 |
| Trial 3 | 17.02714165 | 18.1456743 | 17.27629347 | 15.58524173 | 17.23918575 | 14.7264631 | 18.864 |
| Average | 17.38834473 | 16.66383932 | 17.62852659 | 15.9984829 | 17.59452807 | 14.72627838 | |
| STD | 0.580175753 | 2.614550186 | 0.523839569 | 0.542443325 | 0.524580034 | 0.53098236 | |

**PERCENT ABSORBANCE-NO TOP LAYER**

| Absorbance | 0.3 g/mL | 0.5 g/mL | 0.7 g/mL | 0.9g/mL | 1.1 g/mL | Total |
|---|---|---|---|---|---|---|
| Trial 1 | 20.59863602 | 21.94998737 | 20.9585754 | 19.05152816 | 20.92068704 | 15.836 |
| Trial 2 | 22.03689836 | 16.6519164 | 22.24794064 | 20.27367418 | 22.20709374 | 14.689 |
| Trial 3 | 20.52133913 | 21.86940966 | 20.82162024 | 18.78354204 | 20.77689752 | 15.652 |
| Average | 21.05229117 | 20.15710448 | 21.34271209 | 19.36958146 | 21.30155944 | |
| STD | 0.853570263 | 3.035849269 | 0.786935968 | 0.794349968 | 0.787504377 | |

**ALKALINE ASSAY**

| Absorba | Top | 0.3 g/mL | 0.5 g/mL | 0.7 g/mL | 0.9 g/mL | 1.1 g/mL | Blank |
|---|---|---|---|---|---|---|---|
| Trial 1 | 1.551 | 1.316 | 0.776 | 0.531 | 0.42 | 0.45 | 0.043 |
| Trial 2 | 1.554 | 1.324 | 0.78 | 0.533 | 0.427 | 0.451 | 0.043 |
| Trial 3 | 1.55 | 1.323 | 0.779 | 0.534 | 0.423 | 0.452 | 0.043 |

**SUBTRACTION OF BLANK**

| Absorba | Top | 0.3 g/mL | 0.5 g/mL | 0.7 g/mL | 0.9 g/mL | 1.1 g/mL | Blank |
|---|---|---|---|---|---|---|---|
| Trial 1 | 1.508 | 1.273 | 0.733 | 0.488 | 0.377 | 0.407 | 0 |
| Trial 2 | 1.511 | 1.281 | 0.737 | 0.49 | 0.384 | 0.408 | 0 |
| Trial 3 | 1.507 | 1.28 | 0.736 | 0.491 | 0.38 | 0.409 | 0 |

**PERCENT ABSORBANCE**

| Absorba | Top | 0.3 g/mL | 0.5 g/mL | 0.7 g/mL | 0.9 g/mL | 1.1 g/mL | Total |
|---|---|---|---|---|---|---|---|
| Trial 1 | 31.50857 | 26.59841 | 15.3155 | 10.19641 | 7.877142 | 8.50397 | 4.786 |
| Trial 2 | 31.40719 | 26.62648 | 15.31906 | 10.18499 | 7.981709 | 8.480565 | 4.811 |
| Trial 3 | 31.37622 | 26.65001 | 15.32376 | 10.22278 | 7.911722 | 8.515511 | 4.803 |
| Average | 31.43066 | 26.62497 | 15.31944 | 10.20139 | 7.923524 | 8.500015 | |
| STD | 0.069223 | 0.025832 | 0.004139 | 0.01938 | 0.053273 | 0.017805 | |

**PERCENT ABSORBANCE-NO TOP LAYER**

| Absorba | 0.3 g/mL | 0.5 g/mL | 0.7 g/mL | 0.9g/mL | 1.1 g/mL | Total |
|---|---|---|---|---|---|---|
| Trial 1 | 38.83466 | 22.3612 | 14.88713 | 11.50092 | 12.41611 | 3.278 |
| Trial 2 | 38.81818 | 22.33333 | 14.84848 | 11.63636 | 12.36364 | 3.3 |
| Trial 3 | 38.83495 | 22.3301 | 14.89684 | 11.52913 | 12.40898 | 3.296 |
| Average | 38.82926 | 22.34154 | 14.87749 | 11.55547 | 12.39624 | |
| STD | 0.009598 | 0.017097 | 0.025581 | 0.071463 | 0.028461 | |

Obtained on January 10th, 2018

**DATE: Feb. 10th**

**ACID ASSAY**

| Absorba | Top | 0.3 g/mL | 0.5 g/mL | 0.7 g/mL | 0.9 g/mL | 1.1 g/mL | Blank |
|---|---|---|---|---|---|---|---|
| Trial 1 | 0.985 | 1.559 | 0.758 | 0.707 | 1.316 | 1.579 | 0.043 |
| Trial 2 | 0.993 | 1.58 | 0.76 | 0.71 | 1.329 | 1.907 | 0.043 |
| Trial 3 | 0.838 | 1.267 | 0.701 | 0.596 | 1.337 | 1.669 | 0.043 |

**SUBTRACTION OF BLANK**

| Absorba | Top | 0.3 g/mL | 0.5 g/mL | 0.7 g/mL | 0.9 g/mL | 1.1 g/mL | Blank |
|---|---|---|---|---|---|---|---|
| Trial 1 | 0.942 | 1.516 | 0.715 | 0.664 | 1.273 | 1.536 | 0 |
| Trial 2 | 0.95 | 1.537 | 0.717 | 0.667 | 1.286 | 1.864 | 0 |
| Trial 3 | 0.795 | 1.224 | 0.658 | 0.553 | 1.294 | 1.626 | 0 |

**PERCENT ABSORBANCE**

| Absorba | Top | 0.3 g/mL | 0.5 g/mL | 0.7 g/mL | 0.9 g/mL | 1.1 g/mL | Total |
|---|---|---|---|---|---|---|---|
| Trial 1 | 14.17394 | 22.81071 | 10.75835 | 9.990972 | 19.15438 | 23.11165 | 6.646 |
| Trial 2 | 13.53084 | 21.89147 | 10.21222 | 9.500071 | 18.31648 | 26.54892 | 7.021 |
| Trial 3 | 12.92683 | 19.90244 | 10.69919 | 8.99187 | 21.04065 | 26.43902 | 6.15 |
| Average | 13.54387 | 21.53487 | 10.55659 | 9.494304 | 19.50384 | 25.36653 | |
| STD | 0.623657 | 1.486568 | 0.299693 | 0.499576 | 1.395302 | 1.953561 | |

**PERCENT ABSORBANCE-NO TOP LAYER**

| Absorba | 0.3 g/mL | 0.5 g/mL | 0.7 g/mL | 0.9g/mL | 1.1 g/mL | Total |
|---|---|---|---|---|---|---|
| Trial 1 | 16.51473 | 26.57784 | 12.53506 | 11.64095 | 22.31767 | 5.704 |
| Trial 2 | 15.64816 | 25.31708 | 11.81025 | 10.98666 | 21.18267 | 6.071 |
| Trial 3 | 14.84594 | 22.85714 | 12.28758 | 10.3268 | 24.16433 | 5.355 |
| Average | 15.66961 | 24.91735 | 12.21096 | 10.9848 | 22.55489 | |
| STD | 0.834601 | 1.892282 | 0.368433 | 0.65708 | 1.504919 | |

**ALKALINE ASSAY**

| Absorba | Top | 0.3 g/mL | 0.5 g/mL | 0.7 g/mL | 0.9 g/mL | 1.1 g/mL | Blank |
|---|---|---|---|---|---|---|---|
| Trial 1 | 0.553 | 0.383 | 0.169 | 0.112 | 0.119 | 0.125 | 0.043 |
| Trial 2 | 0.568 | 0.387 | 0.17 | 0.112 | 0.12 | 0.136 | 0.043 |
| Trial 3 | 0.564 | 0.387 | 0.166 | 0.115 | 0.117 | 0.14 | 0.043 |

**SUBTRACTION OF BLANK**

| Absorba | Top | 0.3 g/mL | 0.5 g/mL | 0.7 g/mL | 0.9 g/mL | 1.1 g/mL | Blank |
|---|---|---|---|---|---|---|---|
| Trial 1 | 0.51 | 0.34 | 0.126 | 0.069 | 0.076 | 0.082 | 0 |
| Trial 2 | 0.525 | 0.344 | 0.127 | 0.069 | 0.077 | 0.093 | 0 |
| Trial 3 | 0.521 | 0.344 | 0.123 | 0.072 | 0.074 | 0.097 | 0 |

**PERCENT ABSORBANCE**

| Absorba | Top | 0.3 g/mL | 0.5 g/mL | 0.7 g/mL | 0.9 g/mL | 1.1 g/mL | Total |
|---|---|---|---|---|---|---|---|
| Trial 1 | 42.39401 | 28.26268 | 10.47382 | 5.735661 | 6.317539 | 6.816293 | 1.203 |
| Trial 2 | 42.51012 | 27.85425 | 10.2834 | 5.587045 | 6.234818 | 7.530364 | 1.235 |
| Trial 3 | 42.32331 | 27.94476 | 9.991877 | 5.848903 | 6.011373 | 7.879773 | 1.231 |
| Average | 42.40915 | 28.02056 | 10.2497 | 5.72387 | 6.18791 | 7.40881 | |
| STD | 0.094319 | 0.214505 | 0.242731 | 0.131327 | 0.158382 | 0.54206 | |

**PERCENT ABSORBANCE-NO TOP LAYER**

| Absorba | 0.3 g/mL | 0.5 g/mL | 0.7 g/mL | 0.9g/mL | 1.1 g/mL | Total |
|---|---|---|---|---|---|---|
| Trial 1 | 49.06205 | 18.18182 | 9.95671 | 10.96681 | 11.83261 | 0.693 |
| Trial 2 | 48.4507 | 17.88732 | 9.71831 | 10.84507 | 13.09859 | 0.71 |
| Trial 3 | 48.4507 | 17.32394 | 10.14085 | 10.42254 | 13.66197 | 0.71 |
| Average | 48.65449 | 17.7977 | 9.938622 | 10.74481 | 12.86439 | |
| STD | 0.35296 | 0.435904 | 0.211848 | 0.285655 | 0.936897 | |

Obtained on February 27th, 2018

**Feb. 27th-Day 14 Cells**

**ACID ASSAY**

| Absorba | Top | 0.3 g/mL | 0.5 g/mL | 0.7 g/mL | 0.9 g/mL | 1.1 g/mL | Blank |
|---|---|---|---|---|---|---|---|
| Trial 1 | 1.075 | 1.631 | 1.202 | 1.215 | 0.968 | 2.42 | 0.045 |
| Trial 2 | 1.053 | 1.68 | 1.141 | 0.987 | 0.822 | 1.798 | 0.045 |
| Trial 3 | 1.054 | 1.837 | 1.229 | 1.05 | 0.92 | 1.769 | 0.045 |

**SUBTRACTION OF BLANK**

| Absorba | Top | 0.3 g/mL | 0.5 g/mL | 0.7 g/mL | 0.9 g/mL | 1.1 g/mL | Blank |
|---|---|---|---|---|---|---|---|
| Trial 1 | 1.03 | 1.586 | 1.157 | 1.17 | 0.923 | 2.375 | 0 |
| Trial 2 | 1.008 | 1.635 | 1.096 | 0.942 | 0.777 | 1.753 | 0 |
| Trial 3 | 1.009 | 1.792 | 1.184 | 1.005 | 0.875 | 1.724 | 0 |

**PERCENT ABSORBANCE**

| Absorba | Top | 0.3 g/mL | 0.5 g/mL | 0.7 g/mL | 0.9 g/mL | 1.1 g/mL | Total |
|---|---|---|---|---|---|---|---|
| Trial 1 | 12.4985 | 19.2452 | 14.0396 | 14.1973 | 11.2001 | 28.8193 | 8.241 |
| Trial 2 | 13.9786 | 22.6737 | 15.199 | 13.0634 | 10.7752 | 24.3101 | 7.211 |
| Trial 3 | 13.2956 | 23.6131 | 15.6015 | 13.2429 | 11.5298 | 22.7171 | 7.589 |
| Average | 13.2576 | 21.844 | 14.9467 | 13.5012 | 11.1684 | 25.2822 | |
| STD | 0.74081 | 2.2991 | 0.81098 | 0.60951 | 0.37832 | 3.16512 | |

**PERCENT ABSORBANCE-NO TOP LAYER**

| Absorba | 0.3 g/mL | 0.5 g/mL | 0.7 g/mL | 0.9g/mL | 1.1 g/mL | Total |
|---|---|---|---|---|---|---|
| Trial 1 | 14.2837 | 21.9942 | 16.0449 | 16.2252 | 12.7999 | 7.211 |
| Trial 2 | 16.2502 | 26.3582 | 17.6689 | 15.1862 | 12.5262 | 6.203 |
| Trial 3 | 15.3343 | 27.234 | 17.9939 | 15.2736 | 13.2979 | 6.58 |
| Average | 15.2894 | 25.1955 | 17.2359 | 15.5617 | 12.8747 | |
| STD | 0.984 | 2.80678 | 1.04414 | 0.57631 | 0.39123 | |

**ALKALINE ASSAY**

| Absorba | Top | 0.3 g/mL | 0.5 g/mL | 0.7 g/mL | 0.9 g/mL | 1.1 g/mL | Blank |
|---|---|---|---|---|---|---|---|
| Trial 1 | 0.959 | 0.716 | 0.5 | 0.309 | 0.215 | 0.229 | 0.043 |
| Trial 2 | 0.981 | 0.681 | 0.496 | 0.294 | 0.214 | 0.24 | 0.043 |
| Trial 3 | 1.036 | 0.69 | 0.466 | 0.315 | 0.223 | 0.74 | 0.043 |

**SUBTRACTION OF BLANK**

| Absorba | Top | 0.3 g/mL | 0.5 g/mL | 0.7 g/mL | 0.9 g/mL | 1.1 g/mL | Blank |
|---|---|---|---|---|---|---|---|
| Trial 1 | 0.916 | 0.673 | 0.457 | 0.266 | 0.172 | 0.186 | 0 |
| Trial 2 | 0.938 | 0.638 | 0.453 | 0.251 | 0.171 | 0.197 | 0 |
| Trial 3 | 0.993 | 0.647 | 0.423 | 0.272 | 0.18 | 0.697 | 0 |

**PERCENT ABSORBANCE**

| Absorba | Top | 0.3 g/mL | 0.5 g/mL | 0.7 g/mL | 0.9 g/mL | 1.1 g/mL | Total |
|---|---|---|---|---|---|---|---|
| Trial 1 | 34.3071 | 25.206 | 17.1161 | 9.96255 | 6.44195 | 6.96629 | 2.67 |
| Trial 2 | 35.423 | 24.0937 | 17.1073 | 9.47885 | 6.4577 | 7.43958 | 2.648 |
| Trial 3 | 30.9153 | 20.1432 | 13.1694 | 8.46824 | 5.60399 | 21.6999 | 3.212 |
| Average | 33.5485 | 23.1476 | 15.7976 | 9.30321 | 6.16788 | 12.0352 | |
| STD | 2.34763 | 2.66067 | 2.2761 | 0.76248 | 0.48841 | 8.37316 | |

**PERCENT ABSORBANCE-NO TOP LAYER**

| Absorba | 0.3 g/mL | 0.5 g/mL | 0.7 g/mL | 0.9g/mL | 1.1 g/mL | Total |
|---|---|---|---|---|---|---|
| Trial 1 | 38.3694 | 26.0547 | 15.1653 | 9.80616 | 10.6043 | 1.754 |
| Trial 2 | 37.3099 | 26.4912 | 14.6784 | 10 | 11.5205 | 1.71 |
| Trial 3 | 29.1573 | 19.0626 | 12.2578 | 8.11176 | 31.4105 | 2.219 |
| Average | 34.9456 | 23.8695 | 14.0338 | 9.30597 | 17.8451 | |
| STD | 5.04071 | 4.16861 | 1.55726 | 1.03875 | 11.7569 | |

## *Appendix C: Sucrose Gradient Separation Layers*

A) 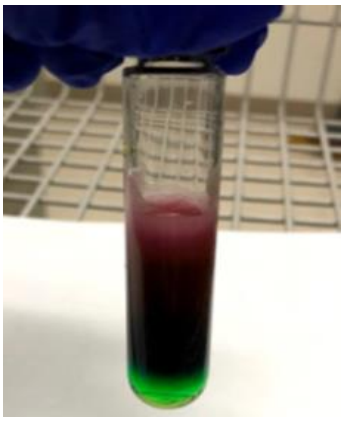

B)